Two-stage stochastic programming for the design optimization of district cooling networks under demand and cost uncertainty

Applied Thermal Engineering 236 (2024) 121594

Contents lists available at ScienceDirect

Applied Thermal Engineering

journal homepage: www.elsevier.com/locate/ate

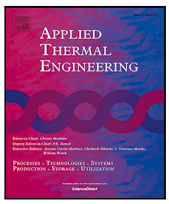

Research Paper

Two-stage stochastic programming for the design optimization of district cooling networks under demand and cost uncertainty

Manfredi Neri *, Elisa Guelpa, Vittorio Verda

Department of Energy DENERG, Polytechnic University of Turin, Italy

ARTICLE INFO

Keywords:
District cooling
Stochastic programming
Design optimization

ABSTRACT

The major limitations of district cooling systems are the high capital costs, which make design optimization tools necessary to maximize the potential benefits. Decision makers when designing district cooling have to handle cost and demand uncertainties that further increase the investment risks. On the other hand, the possible evolution of cooling demand during the years, shall be taken into account in the first design stages, in order to allow network expansion in the future. In this paper, a novel two-stage stochastic programming model is therefore proposed for the optimal design of district cooling networks under demand and cost uncertainty. The model was also applied to a case study and the results showed that it is more convenient to build smaller district cooling networks (and eventually enhance them in the future if the cooling demand and electricity costs will increase) rather than building larger systems from the beginning. In addition, it was found that the uncertainties in electricity cost and cooling demand are the ones that most influence the optimal solution. The impact of the stochastic model was evaluated with respect to deterministic approaches, resulting up to 5% less expensive in terms of expected cost and with a three years lower payback time. A second model formulation was also implemented, with more rigid constraints, which limit the amount of pipes that can be installed in a single branch. With this formulation, the model tends to connect more buildings and to install larger pipes from the beginning, but the solution in terms of expected cost is only 0.4% more expensive than the more flexible one. Lastly, it was analysed the impact of asset residual value at the end of project life, revealing that neglecting it would lead to connecting more buildings initially, but in most scenarios the network would not be expanded in the future.

1. Introduction

Building sector is responsible for 40% of global energy consumptions [1] and 33% of greenhouse gas emissions [2]. In particular, 18% to 73% of building energy consumption is represented by the demand for heating and cooling [3]. The latter has increased by more than twice since 1990, being nowadays responsible for 8.5% of global electricity consumption [4]. In addition, cooling demand during heat waves can reach large peaks that affect the stability of the electrical grid. Demand for space cooling is continuing to rise and currently accounts for 20% of building electricity consumption. Moreover, it is expected that by 2050 more than 60% of households will be equipped with air conditioning systems, since they are becoming more accessible, especially in emerging economies [5]. However, users tend to buy units whose efficiency is about 50% lower compared to the best available technology. According to the International Energy Agency, cooling sector is not on track and requires major interventions in order to reach the sustainable development goals. More actions are required to improve the efficiency of air conditioning systems and to promote energy saving measures such as the implementation of passive cooling solutions or the proper insulation of the building envelope with innovative materials [6]. In this context, solar energy can also be effectively exploited to reduce the electricity demand required for cooling, thanks to the integration with absorption chillers [7,8] or desiccant cooling systems [9].

District cooling represents a suitable alternative to conventional cooling systems, as they are estimated to be 40% more efficient and can lead to 20% reduction of total life-cycle costs [10]. What is more, if integrated with renewable energy sources additional savings can be obtained [11]. In particular, cold water from lakes, rivers or seas can be used to provide free cooling or to increase the efficiency of the chillers [12]. Moreover, waste heat from industrial plants or data centres can be converted into cooling through absorption chillers [13]. Thanks to cold energy storage, district cooling systems can also be used to stabilize the electrical grid using power-to-cool technologies. In these cases the chillers produce cooling power when the demand is

* Corresponding author.
E-mail address: manfredi.neri@polito.it (M. Neri).

https://doi.org/10.1016/j.applthermaleng.2023.121594
Received 4 May 2023; Received in revised form 24 July 2023; Accepted 10 September 2023
Available online 15 September 2023

Nomenclature

Indices

$centr$	Node of the centralized chiller
j	Generic branch of the graph
m	Generic pipe diameter
$s1$	Generic first period scenario
$s2$	Generic second period scenario
t	Used to generalize $t1$ and $t2$
$t1$	First time period
$t2$	Sedond time period
u	Generic building node
v	Generic inner node

Input parameters

ΔT	Temperature difference between supply and return lines (K)
η_{pump}	Pump efficiency (%)
π^{s1}	Probability of scenario $s1$ (%)
ρ	Water density (kg/m^3)
A	Incidence matrix of the graph (nondimensional)
a_{ij}	Generic element of incidence matrix, where i represents a generic node and j an edge of the graph considered (nondimensional)
c_p	Water specific heat [kJ/(kg*K)]
$c^{s1}_{chill,DC}$	Capital cost of centralized chillers per unit of power in scenario $s1$ (€/kW)
$c^{s1}_{chill,ind}$	Capital cost of individual chillers per unit of power in scenario $s1$ (€/kW)
c^{s1}_{el}	Electricity cost in scenario $s1$ (€/kWh)
$c_{ETS,u}$	Capital cost of the energy transfer station in building u (€)
c^{m}_{pipe}	Cost per unit of pipe length, for pipes with diameter m (€/m)
COP_{DC}	Coefficient of performance for centralized chillers (nondimensional)
COP_{ind}	Coefficient of performance for individual chillers (nondimensional)
$Gext_u$	Mass flow rate requested by building u (kg/s)
$incr^{s1}$	Cooling increase rate in scenario $s1$ (%)
L_j	Length of branch j (m)
Nh^{t1}_u	Number of full load hours for building u at year 0 (h)
p_{min}	Minimum pressure in the network (bar)
Q^0_u	Yearly cooling demand of building u at year 0 (kWh)
r	Discount rate (%)
R^m_j	Fluid dynamic resistance per unit of mass flow rate (Pa*s^2/kg^2)

Sets

E	Set of branches of the graph
I	Set of all nodes in the graph
M	Set of pipe diameters
$S1$	Set of first period scenarios
$S2$	Set of second period scenarios
T	Union of first and second stages
U	Set of building nodes
V	Set of inner nodes in the graph

Model variables

$\Delta p^{t2,s1}_j$	Pressure drop in branch j in the second time period if scenario $s1$ occurred (Pa)
Δp^{t1}_j	Pressure drop in branch j in the first time period (Pa)
$G^{t2,s1}_j$	Peak mass flow rates flowing in branch j in time period $t2$ after revelation of scenario $s1$ (kg/s)
G^{t1}_j	Peak mass flow rates flowing in branch j in time period $t1$ (kg/s)
$Gcentr^{t1}$	Mass flow rate flowing from centralized chiller in the first time period (kg/s)
$Gcentr^{t2,s1}$	Mass flow rate flowing from centralized chiller in time period $t2$ if scenario $s1$ occurred (kg/s)
$GpNh^{t1}$	Product between $Gcentr^{t1}$ p^{t1}_{centr} and the initial number of full load operating hours (kg/s*Pa*h)
$GpNh^{t2,s1}$	Product between $Gcentr^{t2,s1}$ $p^{t2,s1}_{centr}$ and the number of full load operating hours at the end of first time period if scenario s1 occurred (kg/s*Pa*h)
p^{t1}_i	Relative pressure at node i in the first time period (Pa)
$p^{t2,s1}_j$	Relative pressure at node i in the second time period, if scenario $s1$ occurred (Pa)
$Size^{t1}_{centr}$	Capacity of centralized chiller installed in the first time period (kW)
$Size^{t2,s1}_{centr}$	Capacity of centralized chiller installed in the second stage if scenario s1 occurred (kW)

lower, that is stored and released when the cooling demand is larger. This strategy allows not only to stabilize the electrical grid, but also to install smaller chillers and reduce operation costs [14]. In district cooling systems, chilled water is produced in one or more central plants through electrical or absorption chillers or by using a natural cooling source, as a large water basin. Through a piping system the chilled water is distributed to the building substations. There the excess heat is transferred to the chilled water, which then returns back to the central plant through the return line [15]. These systems are usually more efficient than individual cooling because they can easily exploit renewable sources and are equipped with larger industrial chillers, which have higher coefficients of performance. Moreover, thanks to the cooling load diversity, the total demand curve is smoother with lower peaks. As a consequence, the chillers in district cooling systems are not oversized and can operate closer to design conditions, with better performances, for most of the time [16].

The temperature difference between supply and return in district cooling systems ranges between 6.7 °C and 11 °C, which is sensibly lower than in district heating systems [17,18]. As a consequence, larger mass flow rates, pipe diameters and pumping power are required. Consequently, the capital and operation expenditures are larger for a district cooling system. For this reason, district cooling is economically feasible in areas with large energy density(e.g thermal demand for squared kilometre of land) [19]. If not properly planned and operated, the advantages of this technology would be limited [20]. Optimization

$Size_{ind,u}^{t1}$	Installed capacity of individual chiller for building u in the first decision stage (kW)
$Size_{ind,u}^{t2,s1}$	Installed capacity of individual chiller for building u in the second decision stage if scenario s1 occurred (kW)
up_{centr}^{t1}	Product between the variables p_{centr}^{t1} and y_u^{t1} (Pa)
$up_{centr}^{t2,s1}$	Product between the variables $p_{centr}^{t2,s1}$ and $y_u^{t2,s1}$ (Pa)
$x_j^{m,t1}$	Binary variable that indicates if the diameter m is selected for branch j in the first time period (nondimensional)
$x_j^{m,t2,s1}$	Binary variable that indicates if the diameter m is selected for branch j in the second stage for scenario $s1$ (nondimensional)
xz_j^{s1}	Auxiliary variable used to linearize the product between x_j^{t1} and z_j^{s1} (nondimensional)
Y_j^{t1}	Inverse of fluid dynamic resistance per unit of mass flow rate in pipe installed in the first stage in branch j (kg*m)
$Y_j^{t2,s1}$	Inverse of fluid dynamic resistance per unit of mass flow rate in pipe installed in branch j in the second stage for scenario $s1$ (kg*m)
y_u^{t1}	Binary variable that indicates weather the user u is connected to the network in the first time period (nondimensional)
$y_u^{t2,s1}$	Binary variable that indicates weather the user u is connected to the network in the second stage if scenario $s1$ occurred (nondimensional)
$z_j^{t2,s1}$	Binary variables that indicate weather a new pipe is installed in branch j in the second stage, if scenario s1 occurred (nondimensional)

tools are therefore necessary to support engineers and decision makers in the planning of district cooling systems in order to minimize the costs and the greenhouse gas emissions.

Different models have been developed and implemented for the optimization of district heating and cooling systems. Concerning operation optimization, different models have been developed to optimize the most impactful variables: the schedule of chillers and storages, the pumps working conditions and the supply temperatures. Powell et al. [21] developed a dynamic programming algorithm to optimize the chillers and storage schedule in district cooling networks. The results showed that thanks to this methodology it is possible to reduce by 9.4% the energy consumption and to save up to 17.4% in terms of electricity expenditures. Wang et al. [22] developed a hybrid model for chiller operation and optimized it with a genetic algorithm. They analysed the impact of each variable on the optimization and proposed flexible search bounds in order to limit the range of the least influencing variables. Zhang et al. [23] proposed an alternative operation strategy consisting in providing a variable chilled water supply temperature. The authors showed that the strategy would allow to reduce electricity consumption by 19%. Chiam et al. [24] developed a hierarchical model to optimize the operation of district cooling systems. The tool is formed by a genetic algorithm at master level and a MILP at inferior level. This model can optimize the whole system and compared to an optimization limited to chillers operation, it allows to achieve further savings. Cox et al. [25] developed a model predictive control strategy coupled with a genetic algorithm to optimize the operation of a district cooling network with thermal storage in real-time. The model allowed to save up to 16% of the operation cost.

Regarding the design optimization of district heating and cooling systems, models are used to optimize the layout, pipe diameters and the position and size of pumps, central plants and storages. Zaw et al. [26] developed an optimization tool, based on the interior point method, to optimize the design and operation of chillers and thermal storages in district cooling networks. They applied their model to the Singapore case study and observed that it would allow to reduce the payback time up to 20%. Mazzoni et al. [27] developed a platform for the master planning of polygeneration systems and their optimal scheduling. By testing the platform on a district cooling case study, they showed that it would achieve up to 30% reduction of capital costs and up to 12% of primary energy savings. Lo et al. [28] implemented a mathematical model to select the optimal pumping configuration in a district cooling system. Compared to a baseline scenario, the optimal setup would allow to reduce the pumping costs by 23%. Guelpa et al. [29] developed a genetic algorithm to optimize the position of chillers in a district cooling network, with the goal of minimizing the costs for piping installation and pumping. Chan et al. [30] implemented a genetic algorithm integrated with a local search approach to optimize the layout of a district cooling network. They started from a graph where the nodes are all connected to each others and determined the spanning tree that minimizes piping and pumping costs. Zeng et al. [31] implemented a genetic algorithm to select the optimal pipe diameters in a district heating and cooling load. Moreover, they performed a sensitivity analysis, which showed that electricity cost has low impact on the optimal pipe sizes. Soderman [32] developed a MILP model to optimize the position of chillers and storage in a district cooling network that connects buildings with different demand profiles. Al-Noaimi et al. [33] implemented a MINLP model to optimize the design of a district cooling system. The objective of their optimization was to select the network layout, the pipe diameters and the locations of chillers and storages. The authors linearized non-linearities using reformulation linearization techniques. The optimization results evidenced the positive impact of thermal energy storage on district cooling systems. Other authors solved the network layout optimization problem using heuristic approximate approaches, such as the minimum spanning tree [34,35] or shortest path algorithms [36]. Others focused on the optimization of the buildings to be connected to a district heating and cooling network. Chow et al. [37] developed a genetic algorithm to find the optimal percentages of different building types that in a district cooling system would maximize the diversity factor and flatten the total demand curve. Bordin et al. [38] optimized the expansion of an existing district heating system with a MILP model. Pressure drops were approximated with piecewise linear functions of mass flow rates, while pumping costs were not considered, but lower and upper bounds were set to the pressure variables.

Most of the existing papers propose models that address the design optimization with the logic “now or never”. Only few authors optimized the long-term planning of a district energy system. Butün et al. [39] proposed an optimization approach for the long-term investment plan of an industrial district. The approach would guarantee savings in operation costs up to 27%. Wirtz et al. [40] developed two multiperiod optimization models for the design of fifth generation district heating and cooling systems(5GDHC). The results showed that these models, compared to a single period one, allow to achieve up to 17% of total cost savings.

Moreover, deterministic design optimization can lead to non-optimal decisions, if real scenarios differ from the initial assumptions made in the design phase. In this context, stochastic optimization models can handle uncertainty and support robust decision making by selecting the solution that works better for the combination of possible scenarios. Gang et al. [41] developed a method for the robust optimal design of district cooling networks, taking into account equipment reliability and the uncertainty of cooling load. Mavromatidis et al. [42]

implemented a two-stage stochastic programming model for the design of a distributed energy system under uncertainty. They considered different sources of uncertainty, such as heat and electricity demands, energy prices, solar radiation and the emission factor of the electrical grid. The model optimized the size and technologies to be installed (1st stage variables) and on the base of the scenario that occurs, it optimizes the operation (2nd stage variables). Lambert et al. [43] developed a multistage stochastic programming model to optimize the design phasing and expansion of a district heating system. Their model addressed the uncertainties related to costs and interest rates. Zhou et al. [44] developed a two-stage stochastic programming model for the optimal design of distributed energy systems. The peculiarity of their model is that the first stage variables are optimized through a genetic algorithm, while the uncertainty and second stage variables are handled through a Monte Carlo method. Stevanato et al. [45] through a two-stage stochastic programming model optimized the long-term sizing of rural microgrid, taking into account uncertainty and load evolution.

None of the existing studies optimize the initial design and the future expansions of a district cooling network while taking into account the possible evolution of cooling demand and the uncertainty of electricity and capital costs, despite this represents a crucial analysis to ensure low costs for such large investments and long life-cycle infrastructure. In addition, the uncertainty linked to demand evolution and electricity cost should be properly handled in order to limit the risk of oversizing or undersizing the whole network. A decision maker should indeed plan a district cooling system also based on the possibility that cooling demand could change in the future. In the cases of demand increase, buildings that initially are not economically feasible to be connected to a district cooling network, in a second stage could be convenient to be connected, due to the higher savings that district cooling would provide. As a consequence, the decision makers should consider the possible future connections and network expansions, already in the first design stage, by installing proper sized pipes.

In this context, this paper proposes a two-stage stochastic model for the optimization of district cooling systems under uncertainty. The developed model optimizes the initial design of a district cooling network while taking into account for future expansion and the uncertainty of different parameters, such as demand increase during the years, capital costs and electricity price. In Section 2 the model is described in detail, while Section 3 presents the case study used to test the model. The main results are presented in Section 4 and discussed in Section 5. Finally, conclusions are drawn in Section 6.

2. Stochastic programming model

The goal of this model is to optimize the design of a district cooling system under uncertainty while taking into account the possible future expansion in different scenarios. The model allows to define the initial network to be installed and the buildings to be connected immediately. In addition, the model takes into account the uncertainty of the main parameters and includes the possibility to enhance the network at a later stage, in case some conditions become particularly convenient for district cooling. The model, therefore manages the risk of installing an oversized network, which would be economically unfeasible, in case of scenarios with lower potential of district cooling(i.e. low cooling demand or low electricity cost). At the same time, the model, considers the effect of a possible increase of district cooling potential in the future. The objective is therefore to provide a network design that can work well in all possible scenarios, as a function of their probability to occur, and enlarge it in a second stage, if conditions are sufficiently convenient. The model is formulated with the two-stage stochastic programming paradigm [46]. This method treats the uncertainty in a deterministic fashion, by assuming that the number of possible scenarios is finite and that their probability of occurrence is known in advance. On the other hand, the values of the uncertain parameters that define the different scenarios are only revealed in a second moment. The goal of a stochastic programming algorithm is to optimize the first stage and second stage variables, minimizing the expected value of the cost function, which in this case is characterized by the sum of capital and operational expenditures. As a consequence, the stochastic programming solution is not optimal for every scenario, but it is the one that works better for the scenarios combination. The first stage variables are selected in order to guarantee robustness to the solution, while the second stage variables give flexibility to the solution. The latter, indeed also called recourse decisions, remediate on the base of the scenario that occurred. In this case, the first stage variables refer to the design decisions to be taken immediately, hence the buildings to be connected and the pipes to be installed from the beginning. On the other hand, the second stage variables refer to the future design decisions to be taken depending on the scenario that will occur. The second stage decisions therefore define how the district cooling network is expanded in each scenario.

2.1. General assumptions

The model has been built under the following assumptions:

- Thermal losses are neglected, due to the limited temperature difference between chilled water and the ground. Hence the difference between supply and return temperature is assumed to be constant.
- The electricity cost and the capital costs for chillers are uncertain in the first stage, but they are revealed in the second decision stage. Indeed when designing a district cooling network the capital costs for equipment are uncertain. From literature, only the ranges of these costs is known. Concerning electricity cost, this is uncertain due to the long-period considered. Over the time, it could change due to a variation in future energy policies or due to a change in energy sources.
- The time horizon is divided in two time periods. The first time period ranges between the first and the second decision stage, while the second time period ranges from the second decision stage to the end of the whole time horizon, as shown also in Fig. 1
- In each time period, the cooling demand increases every year by an uncertain rate.
- In the second stage, at the end of the 1st time period, the cost of chillers, the electricity price and the increase rate of cooling demand over the 1st time period are known. However, the increase rate of cooling demand in the next time period is still uncertain.

As a consequence, in the first design stage, it is decided the initial network to be installed and the buildings to be connected immediately. At the second decision stage, the scenario of the 1st time period is revealed and new decisions are taken on the basis of the conditions of this scenario. On the other hand, at the second decision stage, the second period scenario is still unknown. Hence, the decisions taken at the second stage should exploit the knowledge of what happened in the previous time period, but should also work well for the combination of new scenarios that can arise from then on.

2.2. Scenario generation

The problem is characterized by different uncertain parameters. The scenarios are therefore generated by combining all possible values of all parameters. The uncertainty is present in the cost of electricity, the capital cost of chillers and the yearly increase rate of cooling demand. In this subsection the uncertainty parameter and the generation of the scenarios are described. Since the time horizon is divided into two periods, separated by the 2nd decision stage, two levels of scenarios are defined, depending on when they are revealed. First period scenarios reflect the possible situations that can occur in the first time period. Which of these occurred, is revealed only at the second decision stage.

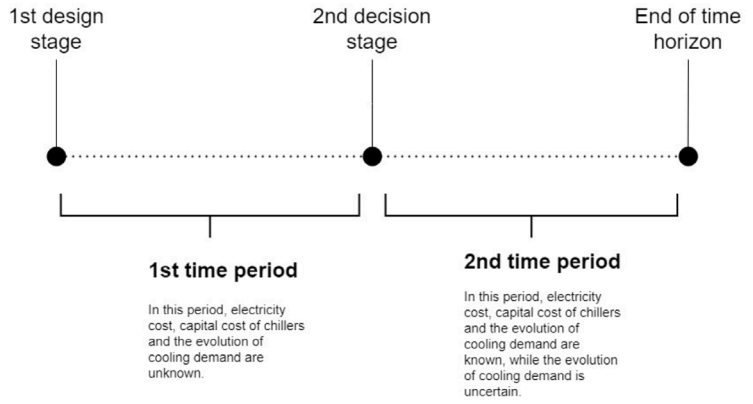

Fig. 1. Time horizon.

Table 1
Values and probabilities for different parameters.

Parameter	Value	Probability
Electricity cost [€/kWh]	[0.1, 0.3, 0.5]	[33.3%, 33.3%, 33.3%]
Demand increase rate [%]	[0, 3, 4]	[25%, 50%, 25%]
Capital cost of centralized chillers [€/kW]	[250, 415, 600]	[33.3%, 33.3%, 33.3%]
Capital cost of individual chillers [€/kW]	[400, 600]	[50%, 50%]

Similarly, second period scenarios indicate the possible situations that can occur in the second time period. Which of the second period scenarios occurred, is revealed only at the end of entire time horizon. Hence, there is no recourse action after the scenario relative to the second period is revealed, since it coincides with the end of project life. The first period scenarios are generated by properly combining all possible values that can be assumed by the parameters that are uncertain in the first stage. Similarly, the second period scenarios are generated by properly combining the possible values that can be assumed by the parameters that are uncertain in the second design stage. The costs of electricity and for the installation of centralized and individual chillers are uncertain in the first stage, but they are revealed in the second stage. The increase rate of cooling demand in the first time period is also unknown and revealed in the second decision stage. In the second design stage it is still uncertain how the cooling demand will change within the second time period.

2.2.1. Cost of electricity

The cost of electricity can sensibly vary due to economical or geopolitical reasons, as observed in 2022 [47]. In this model it is assumed that it varies between 100 €/MWh and 500 €/MWh, with an average of 300 €/MWh. The motivation for these choices is that 100 €/MWh was the average price in 2021, while, the maximum monthly price observed in 2022 was 543 €/MWh [48]. Three possible values were hence considered for scenario generation, representing the average and the lower and upper bounds, as shown in Table 1.

2.2.2. Capital cost of chillers

The capital cost for the installation of chillers is affected by uncertainty, as it can range from 250 to 600 €/kW [49]. Moreover, the cost of manpower influences the installation cost, which therefore is dependent on the country. The model distinguishes two types of chillers: centralized and individual ones. For the first type the cost can vary between 250 and 600 €/kW, while the cost for the second type varies between 400 and 600 €/kW, as shown also in Table 1.

2.2.3. Yearly increase rate of cooling demand

The life-time of the system is assumed to be 30 years. However, this time horizon has been split in two parts in order to be able to enhance the network after the first period, depending on the scenario that shows up. Moreover, the life-time of an individual chiller is typically around 15 years, hence splitting the time horizon in two equal parts results to be a reasonable choice. In this way, if a building is equipped with an individual cooling system, the model decides weather to connect it to a district cooling system only at the end of chiller life-time. In this work it is considered that in each of the two time periods the cooling demand increases with a fixed yearly rate, which however can vary from the first to the second period. The second stage decisions are taken after the scenario relative to the first period is revealed. However, the conditions of the second period are still uncertain when these decisions are taken. In particular, after the second stage decisions are taken, different scenarios may appear, depending on if and how cooling demand increases in the second time period. For both time periods, three different increase rates were chosen with different probabilities, as shown in Table 1. The probability of having a yearly increase rate equal to 3% was set as the highest one. This decision was taken after having evaluated the cooling demand in 2020 and in 2050 in residential buildings. The latter was evaluated using a tool [50] that predicts the variation of the typical meteorological year (TMY), due to climate change. From the analysis it emerged that cooling demand is expected to more than double in the next 30 years. If this demand increase follows an exponential behaviour with a fixed yearly rate, this would be about 3%. The two other values of yearly increase rate(0% and 4%) were added to take into account the uncertain nature of demand increase. It is assumed that in each time period the cooling demand increases with a constant yearly rate. However, this rate could vary between the two time periods. As an example, at first, the cooling demand could increase with a 4% ratio, but in the second time period it could remain stable. All possible evolutions of cooling demand in the two periods are reported in Fig. 2. In thirty years the demand, can therefore either remain constant or increase up to more than two times.

2.2.4. Scenario generation

By combining all the possible parameter values, it results that there are 54 possible scenarios for the first time period, as shown in Fig. 3. At the second decision stage, only the increase of the cooling demand that will occur in the second time period is unknown. Hence, since three possible values have been considered for this parameter, each of the 54 first period scenarios can evolve in three different scenarios in the second time period, for a total of 162 scenarios in the entire time horizon, as shown in Fig. 4.

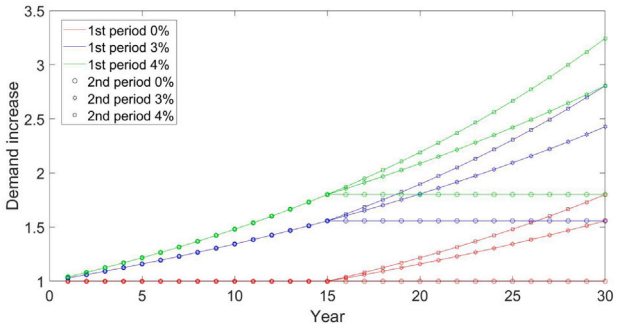

Fig. 2. Possible demand evolutions in the first and second time periods.

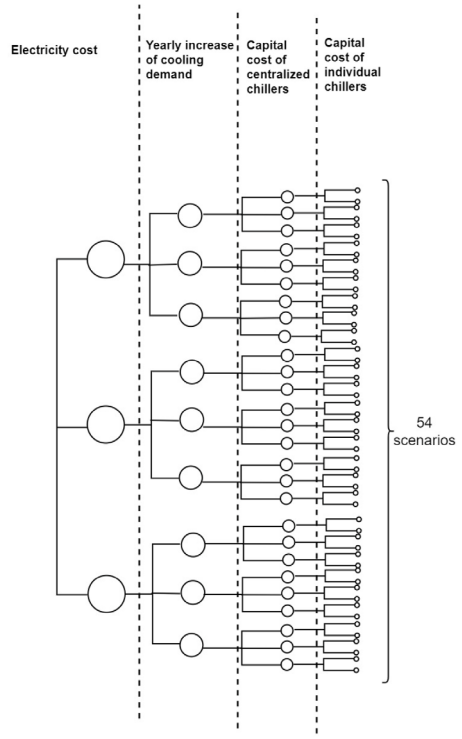

Fig. 3. Definition of 1st period scenarios.

2.3. Input parameters

All the variables and parameters of the model are defined and described in the Nomenclature Section. The values of the input parameters used in the model are defined in Table 2.

2.4. Cost function

In a stochastic programming model the objective is to minimize the expected value of the cost function under all possible scenarios. In this case, the objective function is therefore defined as the sum of investment and operation costs in all possible scenarios, weighted by the probability of scenario occurrence.

$$Obj = Inv^{t1} + \sum_{s1}^{S1} Op^{s1} * \pi^{s1} + \sum_{s1} Inv^{t2,s1} * \pi^{s1} + \sum_{s1}^{S1}\sum_{s2}^{S2} Op^{s1,s2} * \pi^{s1} * \pi^{s2} - Assets_{value} \quad (1)$$

where Inv^{t1} refers to the investments to be taken immediately, $Inv^{t2,s1}$ refers to the cost of investments made in the second decision stage if scenario $s1$ occurred, while π^{s1} and π^{s2} are the probabilities relative to scenarios $s1$ and $s2$. The term Op^{s1} refers to the actualized operation costs relative to the first period, if scenario $s1$ appears, while $Op^{s1,s2}$ refers to the operation costs in the second period, if scenario $s2$ occurs, after the occurrence of scenario $s1$ in the first period. The term $Assets_{value}$ refers to the market value of the assets at the end of the time range. Some of the assets, indeed, are installed in a second moment, hence these will have a residual life-time at the end of the time horizon.

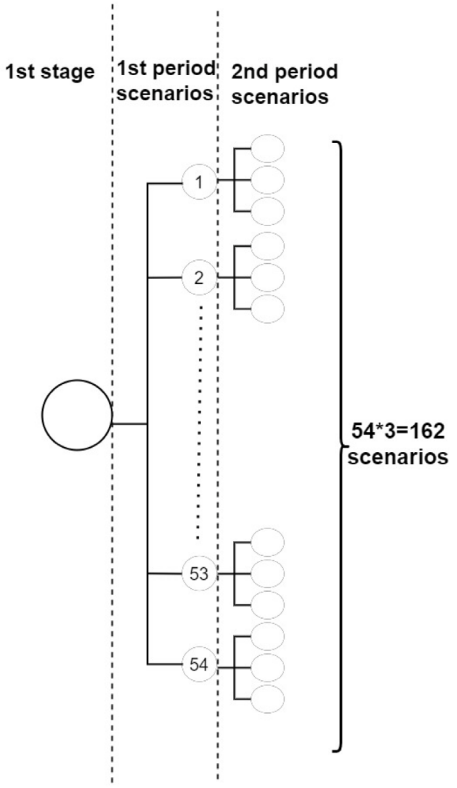

Fig. 4. Generation of 2nd period scenarios.

2.4.1. Investment costs

The investment costs are defined as the sum of the costs for piping, energy transfer stations and chillers.

Piping cost. The piping cost is computed as:

$$Piping^{t1} = \sum_{j}^{E} x_j^{m,t1} * c_{pipe}^{m} * L_j \quad (2)$$

where $x_{ij}^{t1,m}$ is a binary variable equal to 1, if the diameter m is selected for the pipe j. New pipes can be installed also at second stage, depending on the scenario. The investment cost for second stage is defined as:

$$Piping^{t2,s1} = \sum_{j}^{E} x_j^{m,t2,s1} * c_{pipe}^{m} * L_j * \frac{1}{(1+r)^{n_y/2}} \quad (3)$$

where r is the weighted average cost of capital, while $n_y/2$ represents the time difference in years between the first and second decision stage. These parameters are used to actualize the expenditures occurring in the second decision stage.

Energy transfer stations. The cost for energy transfer stations depends on the peak cooling demand requested by the different buildings. This is known, as the demand peak is considered as an input of the problem. Actually, it is unknown if a building is connected to the network or not. This cost therefore depends on the variables y_u^{t1} and $y_u^{t2,s1}$. The cost of

Table 2
Values of main parameters.

Parameter	Value
COP_{DC}	6.5
COP_{ind}	2.5
η_{pump}	0.8
ΔT	7 K
p_{min}	2 bar
r	5%

energy transfer stations installed in the first decision stage is calculated as:

$$cost^{t1}_{ETS} = \sum_{u}^{U} c_{ETS,u} * y^{t1}_{u} \tag{4}$$

where $c_{ETS,u}$ is the cost to install an energy transfer station in building u. Similarly, the cost for energy transfer stations installed in the second stage is defined as:

$$cost^{t2,s1}_{ETS} = \sum_{u}^{U} c_{ETS,u} * y^{t2,s1}_{u} \frac{1}{(1+r)^{n_y/2}} \tag{5}$$

Chiller investment cost. The cost for a centralized chiller installed in the first stage $t1$ is calculated as:

$$Chill^{t1}_{DC} = Size^{t1}_{centr} * \sum_{s1}^{S} c^{s1}_{chill,DC} * \pi^{s1} \tag{6}$$

where $Size^{t1}_{centr}$ defines the capacity of the installed chiller. The terms in the sum represent the average cost per unit of installed capacity, which itself depends on the scenario. Similarly, the capital cost for chiller installed in the second stage, if the generic scenario $s1$ occurs is defined as:

$$Chill^{t2,s1}_{DC} = Size^{t2,s1}_{centr} * c^{s1}_{chill,DC} * \frac{1}{(1+r)^{n_y/2}} \tag{7}$$

The cost for individual chillers installed in the first and second stage is defined as:

$$Chill^{t1}_{ind} = \sum_{u}^{U} Size^{t1}_{ind,u} * \sum_{s1}^{S} c^{s1}_{chill,ind} * \pi^{s1} \tag{8}$$

$$Chill^{t2,s1}_{ind} = \sum_{u}^{U} Size^{t2,s1}_{ind,u} * c^{s1}_{chill,ind} \tag{9}$$

2.4.2. Operation costs

The operation costs consist in the sum of electricity expenditures to power the chillers and the pumps. They are defined as:

$$Op^{s1} = Chill^{s1}_{op,DC} + Chill^{s1}_{op,ind} + C^{s1}_{Pumping} \tag{10}$$

$$Op^{s1,s2} = Chill^{s1,s2}_{op,DC} + Chill^{s1,s2}_{op,ind} + C^{s1,s2}_{Pumping} \tag{11}$$

where:

- $Chill^{s1}_{op,DC}$ and $Chill^{s1,s2}_{op,DC}$ refer to the operating costs of the centralized chillers in the first and second time period according to scenarios $s1$ and $s2$;
- $Chill^{s1}_{op,ind}$ and $Chill^{s1,s2}_{op,ind}$ refer to the operating costs of individual chillers according to scenarios $s1$ and $s2$;
- $C^{s1}_{Pumping}$ and $C^{s1,s2}_{Pumping}$ refer to the pumping cost in the first and second time period according to scenarios $s1$ and $s2$.

Centralized chiller operation. The operating costs of the centralized chiller in the first time period depend on the connected buildings and on the yearly demand increase rate, which itself is different among the scenarios. They are therefore defined as:

$$Chill^{s1}_{op,DC} = \sum_{i=1}^{n_y/2} \sum_{u}^{U} y^{t1}_{u} * Q^{0}_{u} * (1+incr^{s1})^{i} * \frac{c^{s1}_{el}}{COP_{DC}} * \frac{1}{(1+r)^{i}} \tag{12}$$

where Q^0_u is the initial yearly cooling demand, while $incr^{s1}$ and c^{s1}_{el} represents the increase rate and electricity cost in scenario $s1$. Similarly, the operation costs during the second period depend on the cooling demand at the end of the first period and on the increase rate in the new time period. They are defined as:

$$Chill^{s1,s2}_{op,DC} = \sum_{i=n_y/2+1}^{n_y} \sum_{u}^{U} y^{t2,s1}_{u} * Q^{0}_{u} * (1+incr^{s1})^{n_y/2} * (1+incr^{s2})^{i-n_{y2}} * \frac{c^{s1}_{el}}{COP_{DC}} * \frac{1}{(1+r)^{i}} \tag{13}$$

where the product $Q^0_u * (1+incr^{s1})^{n_y/2}$ is the yearly cooling demand of the generic user u at the end of the first time period in scenario $s1$, while $incr^{s2}$ is the demand increase rate in the second period according to scenario $s2$.

Individual chiller operation costs. Similarly, the operation costs for individual chillers in the first and second period are evaluated as:

$$Chill^{s1}_{op,ind} = \sum_{i=1}^{n_y/2} \sum_{u}^{U} (1-y^{t1}_{u}) * Q^{0}_{u} * (1+incr^{s1})^{i} * \frac{c^{s1}_{el}}{COP_{ind}} * \frac{1}{(1+r)^{i}} \tag{14}$$

$$Chill^{s1,s2}_{op,ind} = \sum_{i=n_y/2+1}^{n_y} \sum_{u}^{U} (1-y^{t2,s1}_{u}) * Q^{0}_{u} * (1+incr^{s1})^{n_y/2} * (1+incr^{s2})^{i-n_y/2} * \frac{c^{s1}_{el}}{COP_{ind}} * \frac{1}{(1+r)^{i}} \tag{15}$$

Pumping costs. The pumping energy required to run the pumps is computed as the product between the peak pumping power and the equivalent number of full load hours. The pumping power is proportional to the product between mass flow rate and the pressure drop on the plant node. Since only supply line is modelled, the pressure drops of the return line are taken into account, by incorporating them with the pressure drops of the supply line using the method presented by Sciacovelli et al. [51]. As a consequence, the pressure node variables refer to relative pressure between supply and return line on these nodes, rather than to absolute values. The pumping power which depends therefore on the product between mass flow rate and the pressure difference between supply and return on the plant node is redefined as the product between mass flow rate and plant node pressure in the equivalent network model. A simple quantitative example is shown in Fig. 5 to better explain how this method works. The example presents a network with three nodes, where the pressure drops on all the branches is set to 1 bar. The absolute pressure supplied by the first node is 8 bar, while the return pressure on the same node is 6 bar. By converting the network to the equivalent one, where the return line pressure drops are summed to the supply line ones, it can be observed that the new node pressure values correspond to the pressure differences between supply and return line on the same nodes. Consequently, the pumping cost of the network, which is for the first time period according to scenario $s1$ is defined as:

$$C^{s1}_{pumping} = \sum_{i=1}^{n_y/2} \frac{GpNh^{t1} * (1+incr^{s1})^{i} * c^{s1}_{el}}{\rho * \eta_{pump}} \tag{16}$$

where $GpNh^{t1}$ is the variable that defines the product between the mass flow rate at peak load, the pressure on the central node and the initial number of full load hours, while ρ and η_{pump} refer to the water density, assumed constant, and the efficiency of the pump. Similarly the pumping cost for the second time period, if scenario $s1$ occurred during the first time period and scenario $s2$ for the second one, it is defined as:

$$C^{s1,s2}_{Pumping} = \sum_{i=n_y/2+1}^{n_y} \frac{GpNh^{t2,s1} * (1+incr^{s2})^{i-n_y/2} * c^{s1}_{el}}{\rho * \eta_{pump}} \tag{17}$$

where $GpNh^{t2,s1}$ is the variable that indicates the product between the mass flow rates at peak load and the number of full load hours at the end of the first time period according to scenario $s1$.

2.4.3. Residual value of the assets

The assets with a residual life-time at the end of the second time period are the pipes, the energy transfer stations and the centralized chillers installed in the second decision stage. The market value is therefore evaluated as the half of these investment cost, corrected by the actualization coefficient, as expressed in Eq. (18).

$$Assets_{value} = \frac{Piping^{t2,s1} + cost_{ETS}^{t2,s1} + Chill_{DC}^{t2,s1}}{2} * \frac{1}{(1+r)^{n_y/2}} \tag{18}$$

2.5. Constraints

The model presents capacity, mass balance and pressure balance constraints. They are described in detail in the following subsections.

2.5.1. Mass balance constraints

Constraints (19)–(21) ensure that mass balance is respected for chiller, user and inner nodes respectively.

$$\sum_{j}^{E} a_{centr,j} * G_j^{t(,s1)} + Gcentr^{t(,s1)} = 0 \qquad \forall t \in T, s1 \in S1 \tag{19}$$

$$\sum_{j}^{E} a_{u,j} * G_j^{t1} + G_{ext,u} * y_u^{t(,s1)} = 0 \qquad \forall t \in T, s1 \in S1, u \in U \tag{20}$$

$$\sum_{j}^{E} a_{v,j} * G_j^{t(,s1)} = 0 \qquad \forall v \in V, t \in T, s1 \in S1 \tag{21}$$

where the apex $t(,s1)$ is used to generalize the apices $t1$ and $t2,s1$ relative to first and second stage variables. This is done to avoid rewriting the equations twice and to ease the readability of the paper. The generic term a_{ij}, present in the three equations, refers to the element of the incidence matrix that tells if the node i is an inlet or an outlet for branch j. The subscripts $centr$, u and v refer to the index relative to the chiller node, the generic user node and the generic inner node.

2.5.2. Capacity constraints

Constraint (22) ensures that no more than a pipe diameter is selected for each pipe.

$$\sum_{m}^{M} x_j^{m,t(,s1)} \leq 1 \qquad \forall j \in E, t \in T, s1 \in S1 \tag{22}$$

Constraint (23) defines the variable $z_j^{t2,s1}$. It is equal to one if a pipe is installed in the second stage. Otherwise, it is forced to be null.

$$\sum_{m}^{M} x_j^{m,t2,s1} = z_j^{t2,s1} \qquad \forall j \in E, t \in T, s1 \in S1 \tag{23}$$

Constraint (24) indicates that in the first time period the mass flow rate in every pipe must not be larger than the maximum allowed by the selected diameter. The maximum mass flow rate indeed depends on the diameter and on the velocity limit, which is assumed equal to 1.5 m/s, coherently with ASHRAE standards [17].

$$\sum_{m}^{M} Gmax^m * x_j^{m,t1} \geq G_j^{t1} \qquad \forall j \in E \tag{24}$$

The capacity constraint must be respected also for the second time period variables, but two different situations may arise:

- the pipe installed in the first stage can work also for the second time period
- capacity of the pipe installed in the first stage is not sufficient

In the second situation, the capacity problem is solved by adding a parallel pipe on the same branch. The mass flow rate is therefore divided in two pipes. It is assumed that the pipe installed in the first stage is exploited to the maximum capacity. This means that the mass flow rate that flows in there is the maximum admissible, while the remaining stream flows in the new installed pipe. This hypothesis is not optimal, but it allows to minimize the size of the new pipes to be installed. Constraint (25) ensures that the mass flow rate in every branch in the second time period must respect the total capacity of the pipes installed.

$$\sum_{m}^{M} Gmax^m * x_j^{m,t1} + \sum_{m}^{M} Gmax^m * x_j^{m,t2,s1} \geq G_j^{t2,s1} \qquad \forall j \in E, s1 \in S1 \tag{25}$$

Constraint (26) ensures that the mass flow rate flowing in the new pipe does not exceed its maximum capacity.

$$Gdiff_j^{s1} - \sum_{m}^{M} Gmax^m * x_j^{m,t2,s1} \leq 0 \qquad \forall j \in E, s1 \in S1 \tag{26}$$

where $Gdiff^{s1}$ is the mass flow rate that flows in the new pipe. Constraint (27) is a big-M constraint that forces $Gdiff^{s1}$ to be equal to the difference between $G_j^{t2,s1}$ and the maximum mass flow rate that can flow in the pre-existing pipe if a new pipe is installed in the second stage.

$$-Gdiff_j^{s1} + G_j^{t2,s1} - \sum_{m}^{M} x_j^{m,t1} * Gmax^m \leq (1 - z_j^{t2,s1}) * B \quad \forall j \in E, s1 \in S1 \tag{27}$$

where B is a sufficiently large number.

Constraints (28) and (29) fix a lower bound on the size of the chiller to install in the first and second stage. It is specified that it should be at least equal to 80% of the sum of demand peaks. This is reasonable since it is unlikely that all users have a demand peak in the same instant. It is therefore assumed that there is a diversity factor of 80%.

$$Size_{centr}^{t1} \geq 0.8 * Gcentr^{t1} * c_p * \Delta T \tag{28}$$

$$Size_{centr}^{t1} + Size_{centr}^{t2,s1} \geq 0.8 * Gcentr^{t2,s1} * c_p * \Delta T \qquad \forall s1 \in S1 \tag{29}$$

Individual chillers have a smaller life-cycle equal to 15 years, hence in the second stage new chillers must be installed for buildings not connected to the network. The size of individual chillers is instead defined by constraint (30).

$$Size_{ind,u}^{t(,s1)} = Gext_u * (1 - y_u^{t(,s1)}) * c_p * \Delta T \qquad \forall u \in U, t \in T, s \in S1 \tag{30}$$

2.5.3. Pressure drop constraints

Constraint (31) defines the variable $Y_j^{t(,s1)}$ as the inverse of fluid dynamic resistance per unit of mass flow rate. In order to avoid values equal to zero, the variable is forced to be equal to 1, if no pipe is installed on the branch j.

$$Y_j^{t(,s1)} = 1 + \sum_{m}^{M} x_j^{m,t(,s1)} * (\frac{1}{R_j^m} - 1) \qquad \forall j \in E, t \in T, s \in S1 \tag{31}$$

Constraint (32) links the pressure drop variables with the relative pressures at inlet and outlet nodes of every branch.

$$\Delta p_j^{t(,s1)} = \sum_{i}^{I} a_{ij} * p_i^{t(,s1)} \qquad \forall j \in E, t \in T, s1 \in S1 \tag{32}$$

The pressure drops in the first time period are defined with the following non-linear equation:

$$\Delta p_j^{t1} = G_j^{t1^2} / Y_j^{t1} \qquad \forall j \in E \tag{33}$$

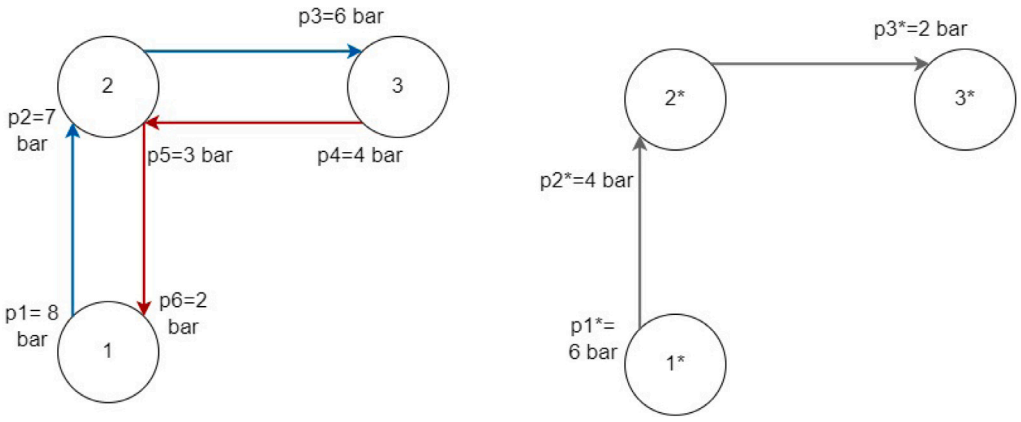

Fig. 5. Quantitative example on the equivalent network method.

For the second time period, due to the possible presence of multiple pipes in parallel on the same branch, it is selected the highest pressure drop. This is guaranteed by constraints (34)–(36).

$$\Delta p_j^{t2,s1} \geq Gdiff_j^{s1\,2}/Y_j^{t2,s1} \qquad \forall j \in E, s1 \in S1 \qquad (34)$$

$$\Delta p_j^{t2,s1} \geq \sum_m^M (Gmax^{m2} * R_j^m * x_j^{m,t1}) * z_j^{t2,s1} \qquad \forall j \in E, s \in S1 \qquad (35)$$

$$\Delta p_k^{t2,s1} \geq G_j^{t2,s1\,2}/Y_j^{t1} * (1 - z_j^{t2,s1}) \qquad \forall j \in E, s1 \in S1 \qquad (36)$$

If no pipe is installed in the second decision stage, constraints (34) and (35) indicate only that $\Delta p_j^{t2,s1}$ is greater than zero. The pressure drop is therefore computed considering that the whole mass flow rate flows in the pre-existing pipe. On the other hand, if a pipe is installed in the second decision stage, the right hand side of constraint (36) is forced to be equal to zero.

The non-linearities in constraints (33) and (34) have been handled by means of the cutting plane method, as done in a previous work by Neri et al. [52]. Since they are convex expressions for positive values of Y_j^{t1} and $Y_j^{t2,s1}$, they can be linearized by solving the problem iteratively and adding the following new constraints at each iteration.

$$\Delta p_j^{t1} \geq 2 * \frac{G_j^{t1\prime}}{Y_j^{t1\prime}} * G_j^{t1} - \frac{G_j^{t1\prime 2}}{Y_j^{t1\prime 2}} * Y_j^{t1} \qquad \forall j \in E \qquad (37)$$

$$\Delta p_j^{t2,s1} \geq 2 * \frac{Gdiff_j^{s1\prime}}{Y_j^{t2,s1\prime}} * Gdiff_j^{t1} - \frac{Gdiff_j^{s1\prime 2}}{Y_j^{t1\prime 2}} * Y_j^{t1} \qquad \forall j \in E, s1 \in S1 \qquad (38)$$

where the apex $\prime$ refers to the solution of the previous iteration.

Constraint (35) is linearized by using the technique to linearize the product of binary variables. Auxiliary variables $xz_j^{m,s1}$ are therefore introduced to substitute the product between $x_j^{m,t1}$ and $z_j^{t2,s1}$. Moreover the following constraints are introduced to guarantee that this equality is respected.

$$xz_j^{m,s1} \geq x_j^{m,t1} + z_j^{t2,s1} - 1 \qquad \forall j \in E, m \in M, s1 \in S1 \qquad (39)$$

$$xz_j^{m,s1} \leq x_j^{m,t1} \qquad \forall j \in E, m \in M, s1 \in S1 \qquad (40)$$

$$xz_j^{m,s1} \leq z_j^{t2,s1} \qquad \forall j \in E, m \in M, s1 \in S1 \qquad (41)$$

Constraint (36) is linearized in two steps. The expression, is indeed similar to that of constraints (33) and (34), which are linearized with the cutting plane method. However, the expression includes also the product with a binary variable. An auxiliary variable $Gz_j^{t2,s1}$ is therefore introduced to substitute the product between $G_j^{t2,s1}$ and $z_j^{t2,s1}$. Moreover the following constraints are added in order to guarantee that this equality is satisfied.

$$Gz_j^{t2,s1} \geq G_j^{t2,s1} + Gmax * z_j^{t2,s1} - Gmax \qquad \forall j \in E, s1 \in S1 \qquad (42)$$

$$Gz_j^{t2,s1} \leq G_j^{t2,s1} \qquad \forall j \in E, s1 \in S1 \qquad (43)$$

$$Gz_j^{t2,s1} \leq Gmax * z_j^{t2,s1} \qquad \forall j \in E, s1 \in S1 \qquad (44)$$

Finally, constraint (36) was linearized with the cutting plane method as shown in (45):

$$\Delta p_j^{t2,s1} \geq 2 * \frac{Gz_j^{t2,s1\prime}}{Y_j^{t1\prime}} * Gz_j^{t2,s1} - \frac{Gz_j^{t1\prime 2}}{Y_j^{t1\prime 2}} * Y_j^{t1} \qquad \forall j \in E, s1 \in S1 \qquad (45)$$

The final model is completely non-linear and can be therefore solved iteratively with a linear solver, such as Gurobi or CPLEX. The stopping criteria used to terminate the iterations is the error in the evaluation of relative pressure on the central node, with a tolerance of 100 Pa.

2.5.4. Pumping energy

The cost function includes also pumping costs, defined in Eqs. (16) and (17). These depend on the variables $GpNh^{t1}$ and $GpNh^{t2,s1}$, which represent the product between the mass flow rate flowing in the network, the pressure at central node and the number of full load hours. They are therefore defined through non-linear relations and need to be linearized.

$$GpNh^{t1} = p_{centr}^{t1} * \sum_u^U Gext_u * Nh_u^{t1} * y_u^{t1} \qquad (46)$$

$$GpNh^{t2,s1} = p_{centr}^{t2,s1} * \sum_u^U Gext_u * Nh_u^{t1} * (1 + incr^{s1})^{n_y/2} * y_u^{t2,s1} \qquad (47)$$

where Nh_u^{t1} is the initial number of full load hours for building u in year 0. These variables depend on the product between continuous and binary variables, hence they can be linearized by introducing additional variables up_{centr}^{t1} and $up_{centr}^{t2,s1}$ that substitute these products. Moreover the following additional constraints must be added as well to ensure that $up_{centr}^{t,(s1)}$ is equal to the product $y_u^{t,(s1)} * p_{centr}^{t,(s1)}$.

$$up_{centr}^{t,(s1)} \geq y_u^{t,(s1)} * p_{min} \qquad \forall u \in U, t \in T, s1 \in S1 \qquad (48)$$

$$up_{centr}^{t,(s1)} \geq p_{centr}^{t,(s1)} + y_u^{t,(s1)} * p_{max} - p_{max} \qquad \forall u \in U, t \in T, s1 \in S1 \qquad (49)$$

$$up_{centr}^{t,(s1)} \leq y_u^{t,(s1)} * p_{min} + p_{centr}^{t,(s1)} - p_{min} \qquad \forall u \in U, t \in T, s1 \in S1 \qquad (50)$$

2.6. Rigid model formulation

In the model described in the previous section, it was assumed that in the second stage new pipes can be installed in the same branches where there already pipes installed in the first stage. The model therefore allows to have multiple pipes in parallel in the same branch. This

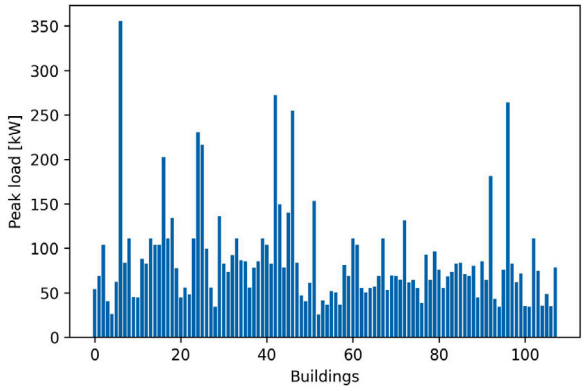

Fig. 6. Buildings peak loads.

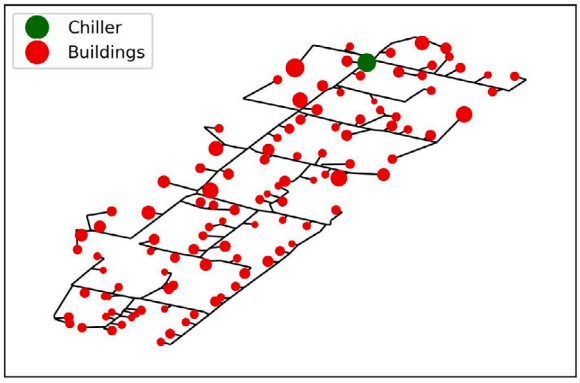

Fig. 7. Topology of case study.

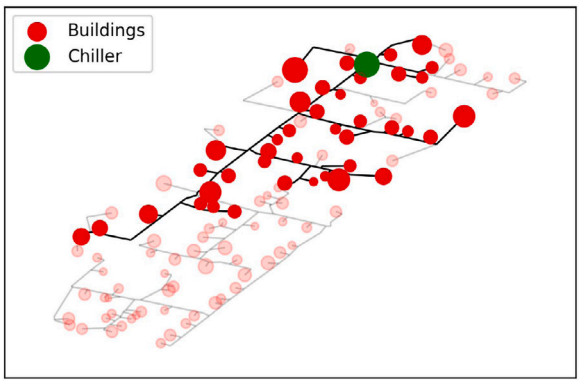

Fig. 8. Optimal first stage network design.

assumption may not be applicable in reality, since there may not be enough space in the ground to install additional pipes close to the existing ones. Hence, a variant formulation has been implemented as well, in which it is avoided the installation of more than one pipe in the same branch of the network. This variant of the original model will be defined from now on as "rigid model", since compared to the previous one guarantees less flexibility. Indeed, due to the different constraints, the network can be enlarged installing new pipes, but the flow capacity of existing branches cannot be increased in the second decision stage.

3. Case study

Both versions of the model have been tested on a case study representing the topology of an existing district heating network connecting 108 buildings in an Italian residential neighbourhood, whose peak cooling loads are reported in Fig. 6. Although it refers to the topology of a district heating network, it represents a realistic application of a district cooling network in Mediterranean areas. Indeed, the shape of a district heating network would be similar to the one of a district cooling system in the same area, since both are designed and built under the same urban limitations. Fig. 7 shows the topology and the position of buildings and the centralized chiller. The network is characterized by 304 nodes and 303 branches. Moreover, the size of the circles in the figure is proportional to the volume of the buildings. The cooling demand of these buildings has been computed by means of a model for transient simulations and the resulting total cooling power required by all buildings is 9.4 MW. In the model it is assumed that the peak power does not increase, hence the yearly demand increases because of a rise in the number of operational hours. The objective of the model is to find which users shall be connected immediately to a district cooling system while taking into account the possible future expansion of the network.

4. Results

In this section are presented the main results obtained by applying the two model formulations to the case study. In the first part the results relative to the flexible formulation are presented, while the ones obtained with the rigid model are presented in a subsection. The flexible model converged after 22 h using a 2.10 GHz Intel(R) Xeon(R) Gold 6230R CPU. Fig. 8 shows the network that should be installed immediately, result of the decisions to be taken at 1st stage. It should be connected to 40 buildings, with a total capacity of 4.77 MW. In the second stage, depending on the scenario, the network can remain as it is or be enlarged. Depending on the scenario, in the second decision stage the network can remain unchanged or be expanded in 23 different ways. Fig. 9 shows few of the possible network enhancements in the second stage with piping details. It should be noted that since in the second stage in some branches an additional pipe has been installed, the ones reported in the figure refer to equivalent pipe sizes. These correspond to the size of pipes that have a flow area equal to the total one.

These results evidence that it is more convenient to install a smaller network at the initial stage and to enlarge it in the future, if conditions are good enough (e.g. higher cost of electricity and larger increase rate of cooling demand). This allows to reduce the risks related to the uncertainties. Indeed it is avoided the realization of a larger investment from the beginning, that could result non convenient, if cooling demand or electricity price does not increase in the future. In fact, if a larger network is built already from the first stage and the cooling demand does not increase or the electricity cost is lower than expected, the higher initial investment costs would not be compensated by sufficient operation savings. As a consequence, the total costs would be larger than the ones obtained by realizing a smaller network and installing individual cooling systems in the remaining buildings.

Fig. 10 compares the solution obtained with the stochastic approach and two obtained deterministically considering the scenarios with the lowest(lowest cost of electricity, lowest increase rate of cooling demand, lowest capital cost of individual chillers, highest capital cost of centralized chillers) and highest potential(highest cost of electricity, highest increase rate, highest capital cost of individual chillers, lowest capital cost of centralized chillers) of district cooling. The graph shows how these solutions behave in the different scenarios. The three curves do not have the same profile, since moving from a scenario to another one may have a positive impact on a solution, while a negative or negligible one on the others. Moreover, in order to make the graph more readable, the scenarios are sorted to give a monotonic stochastic curve.

It can be observed that the stochastic solution is the most robust, as it tends to work well for all possible scenarios, while the other two

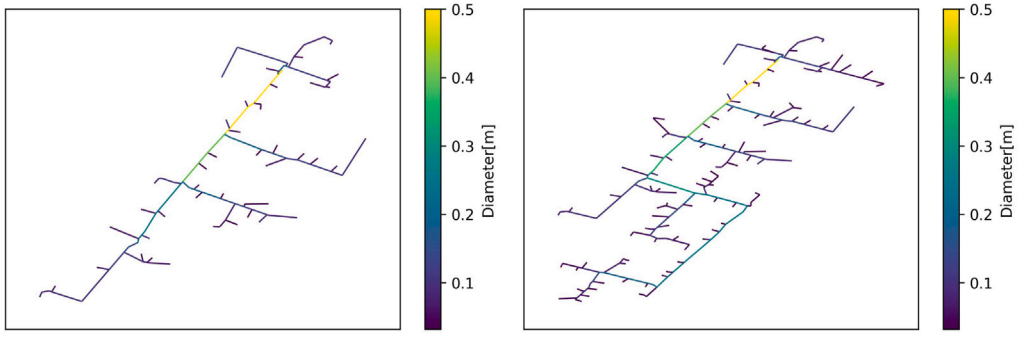

(a) c_{el}=0.10€/kWh, $incr$=0%, $c_{chillIDC}$=250 €/kW, $c_{chill,ind}$=600 €/kW (b) c_{el}=0.50€/kWh, $incr$=0%, $c_{chillIDC}$=250 €/kW, $c_{chill,ind}$=600 €/kW

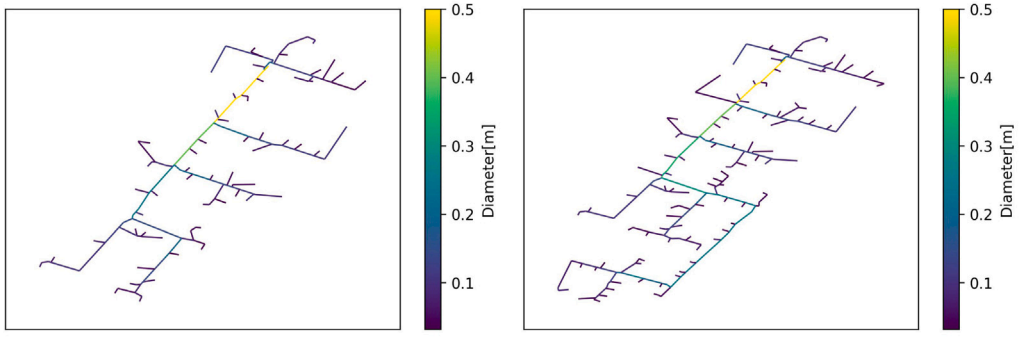

(c) c_{el}=0.50€/kWh, $incr$=3%, $c_{chillIDC}$=416 €/kW, $c_{chill,ind}$=400 €/kW (d) c_{el}=0.50€/kWh, $incr$=4%, $c_{chillIDC}$=600 €/kW, $c_{chill,ind}$=600 €/kW

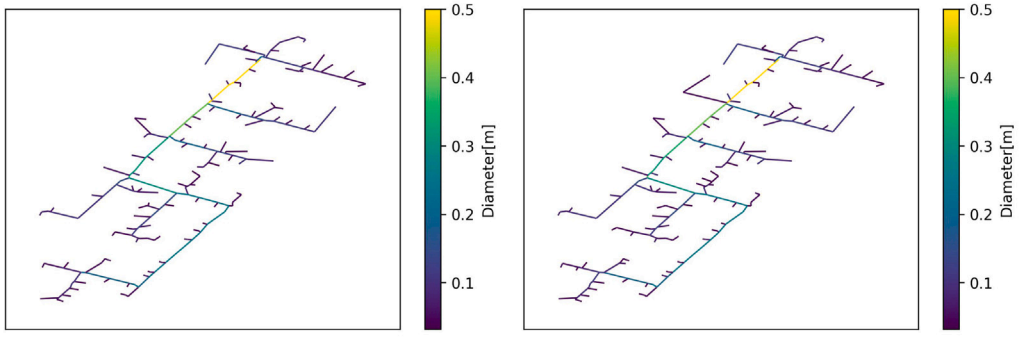

(e) c_{el}=0.30€/kWh, $incr$=3%, $c_{chillIDC}$=250 €/kW, $c_{chill,ind}$=400 €/kW (f) c_{el}=0.30€/kWh, $incr$=4%, $c_{chillIDC}$=600 €/kW, $c_{chill,ind}$=600 €/kW

Fig. 9. Subset of possible second stage network designs in different scenarios.

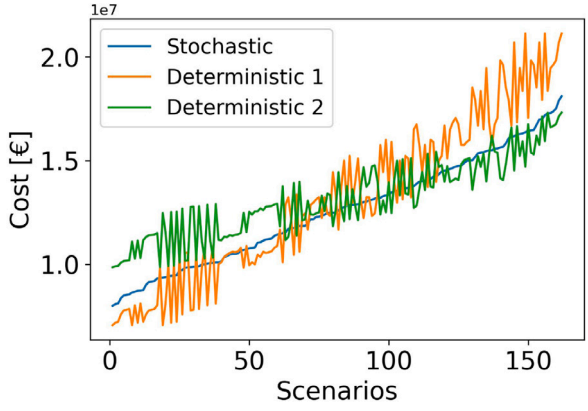

Fig. 10. Comparison between stochastic and deterministic solutions.

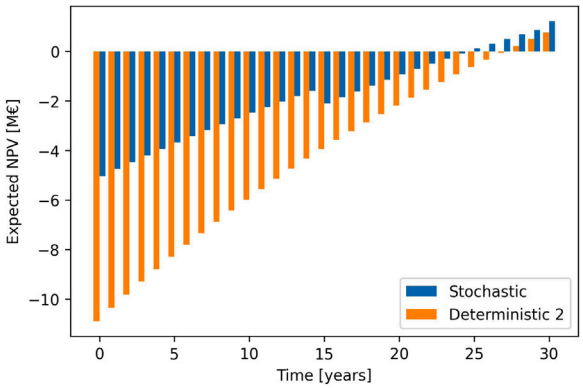

Fig. 11. Net Present Value and payback time analysis.

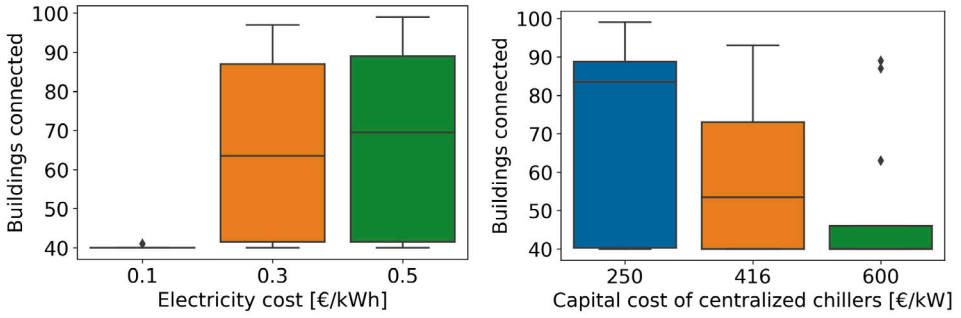

(a) Relation between the number of connected users and the cost electricity

(b) Relation between the number of connected users and the capital cost of centralized chillers

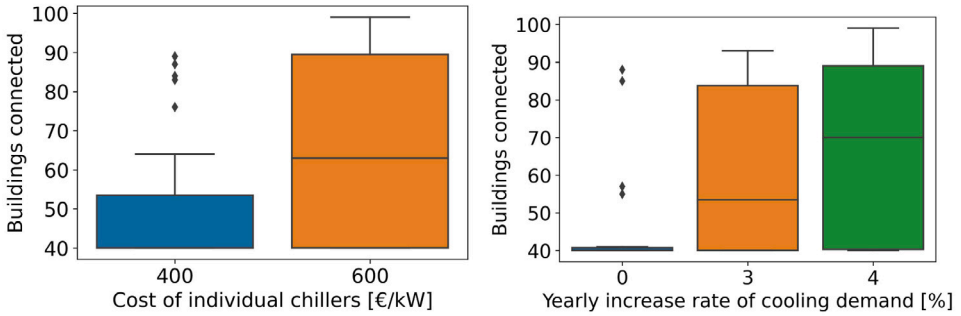

(c) Relation between the number of connected users and the capital cost of individual chillers

(d) Relation between the number of connected users and the demand increase rate

Fig. 12. Influence of the different parameters on the results.

tend to be optimal only in few cases. In particular, in the solution *Deterministic 1*, which was obtained considering the scenario with the lowest potential for district cooling, the total cost is lower compared to the stochastic solution, only in scenarios characterized by a lower cost of electricity and cooling demand. In particular, in the scenario characterized by minimum cost of electricity, cooling demand, cost of individual chillers and maximum cost of centralized chillers, this solution is 24% less expensive than the stochastic one. On the other hand, in scenarios with larger values of electricity cost and cooling demand, the total cost can be up to 29% larger than the one obtained with the stochastic solution. The solution *Deterministic 1* is characterized by the highest range of overall cost variation. In this solution all the buildings are cooled individually and no network is installed. As a consequence this solution provides the lowest overall costs in the scenarios with lower electricity costs and cooling demand. However, for scenarios with larger electricity cost and higher increase rate of cooling demand, the total costs of this solution are the highest, compared to the other two solutions, due to larger operating costs. On the other hand, the solution *Deterministic 2* is the one with the lowest magnitude of cost variation, due to the larger network installed, which increases the capital costs, while reducing the operating ones thanks to the larger efficiency of district cooling compared to individual chillers. This solution tends to work slightly better than the stochastic one in scenarios characterized by higher district cooling potential. In the best case, this solution is 10% less expensive than the stochastic one. However, in scenarios where district cooling is less convenient, the cost can be up to 33% larger compared to the stochastic solution. Indeed, due to the higher number of buildings connected to the network, capital costs are larger, but the savings achievable by district cooling are lower and not sufficient, when electricity cost and cooling demand are lower.

The expected value of the cost function, evaluated for the three different solutions in all possible scenarios is reported in Table 3. As a consequence, the stochastic solution is, on average, up to 5% less expensive than a deterministic one. Fig. 11 shows the expected net present value and payback time for the stochastic and *Deterministic 2* solutions. Solution *Deterministic 1* was not included in the analysis since it corresponds to the case where all the buildings are cooled individually and no district cooling network is installed. The analysis has been carried out considering that the district cooling utility sells chilled water at a price that is dependent on the scenario and corresponds to the cost the users would pay if they installed individual cooling systems. It can be observed that the expected payback time of the stochastic solution is 25 years, while for the solution *Deterministic 2* is 28 years. In addition, the final expected value of net present value of the stochastic solution is 58% larger, with an initial capital investment 54% lower.

Table 3
Expected value of cost function evaluated with the different solutions.

Solution	Expected value of cost fun. [M€]
Stochastic(flexible)	12.63
Deterministic 1	13.28
Deterministic2	13.19
Stochastic (rigid)	12.68

4.1. Impact of parameters uncertainty

In this subsection it is analysed how the uncertainty of the different parameters influences the optimal solution. Fig. 12 shows the number of buildings connected in the second stage(including the ones already connected in the first stage), as a function of the uncertain parameters that are revealed after the first time period.

4.1.1. Electricity cost

The electricity cost has a strong impact on the results. Among the eighteen scenarios with an electricity cost of 0.10 €/kWh, in fifteen of these, no further buildings shall be connected in the second stage. Moreover, in the other three scenarios, only one new building is connected in the second stage. On the other hand, if the electricity cost is equal to 0.3 €/kWh, in 50% of the cases more than twenty-three buildings

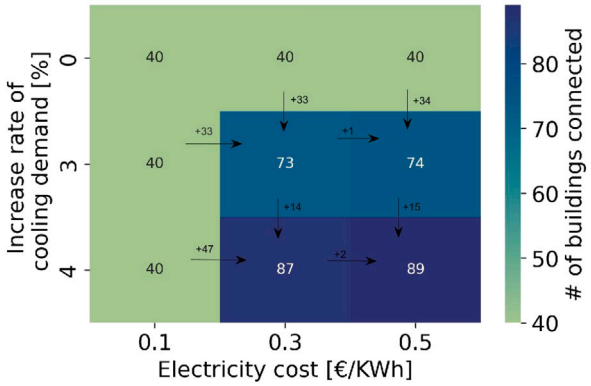

Fig. 13. Combined impact of electricity cost and cooling demand.

should be connected in the second stage. Lastly, with an electricity cost of 0.5 €/kWh, in half of the scenarios more than 30 new connections should be added in the second decision stage.

4.2. Capital cost of centralized chillers

Among the eighteen scenarios with a capital cost of centralized chillers equal to 250 €/kW, in ten of these more than 43 additional buildings shall be connected in the second stage. On the other hand, with a cost of 416 €/kW this happens only in four scenarios. With a capital cost of 600 €/kW, in 50% of the cases, one new building would be connected at most.

4.3. Capital cost of individual chillers

Among the twenty-seven scenarios with a capital cost of individual chillers equal to 400 €/kW, in seventeen of these, no additional buildings shall be connected to the network in the second stage. On the other hand, in twelve cases, more than ten buildings shall be connected. If this cost is equal to 600 €/kW, in twelve cases, more than 43 buildings shall be connected in the second stage.

4.4. Yearly demand increase

In thirteen of the eighteen scenarios in which cooling demand does not increase during the first time period, no new buildings shall be connected in the future. In 56% of the scenarios in which the yearly demand increase rate is equal to 3% in the first time period, at least ten new buildings must be connected to the network in the second stage. Lastly, in nine out of the eighteen scenarios characterized by an increase rate of 4% during the first period, more than 30 new buildings shall be connected in the second stage.

4.4.1. Combined impact of electricity cost and cooling demand increase rate

In Fig. 13 shown a heat map that presents the combined impact of electricity cost and cooling demand increase rate is shown. The values reported in the heat map table, represent the median number of total buildings connected in the second stage (including the ones already connected in the first stage), in all scenarios characterized by those values of electricity cost and cooling demand increase rate. Both parameters have a large impact. In particular, highest differences are observed when varying the increase rate of cooling demand. However, if electricity cost is minimum, the network would remain as it is regardless of the cooling demand increase. The same applies, if cooling demand does not increase during the first time period, regardless of the electricity cost.

Table 4
Parameters used for model validation.

Parameter	Value
Demand increase rate	4%
Electricity cost	0.15 €/kWh
Cost of individual chillers	600 €/kW
Cost of centralized chillers	250 €/kW

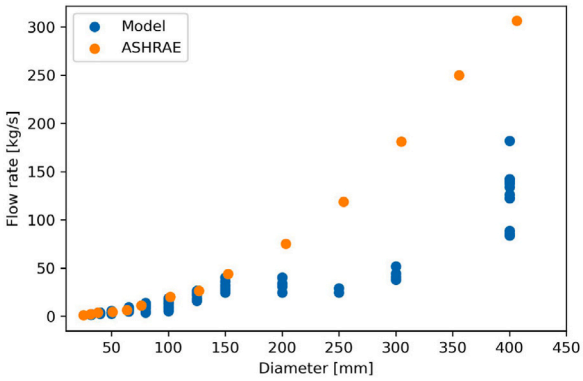

Fig. 14. Pipe capacity: comparison with ASHRAE.

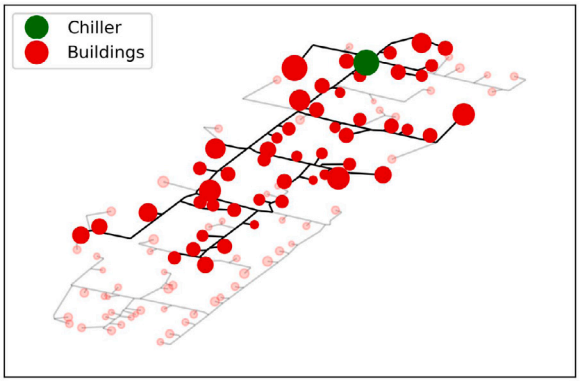

Fig. 15. Network that should be installed from the beginning according to rigid model version.

4.5. Model validation

In order to validate the model, ASHRAE guidelines [53] have been compared to the results of a deterministic scenario, with the characteristics reported in Table 4. In Fig. 14 the mass flow rates flowing in each pipe have been compared with the reference ones reported by ASHRAE. From the figure it can be observed that for smaller diameters, the model tends to have similar results. For diameters larger than 150 mm, the differences are higher and the model tends to select larger diameter for the same mass flow rate. However, these differences may depend on the different parameters used for the analysis, such as the piping costs. In addition, the model for the same mass flow rate, may select a different diameter, depending on the pipe position in the network. Indeed some branches are more critical than others, as they are needed to connect the plant to the farthest buildings. Larger pressure differences can be admissible on the pipes outside of the critical path as far as they do not influence the supply pressure requirements. As a consequence, in these branches, smaller diameters can be installed, allowing to reduce capital costs, without increasing pumping costs. In general, the model is coherent with ASHRAE guidelines, although being more conservative in the choice of diameters.

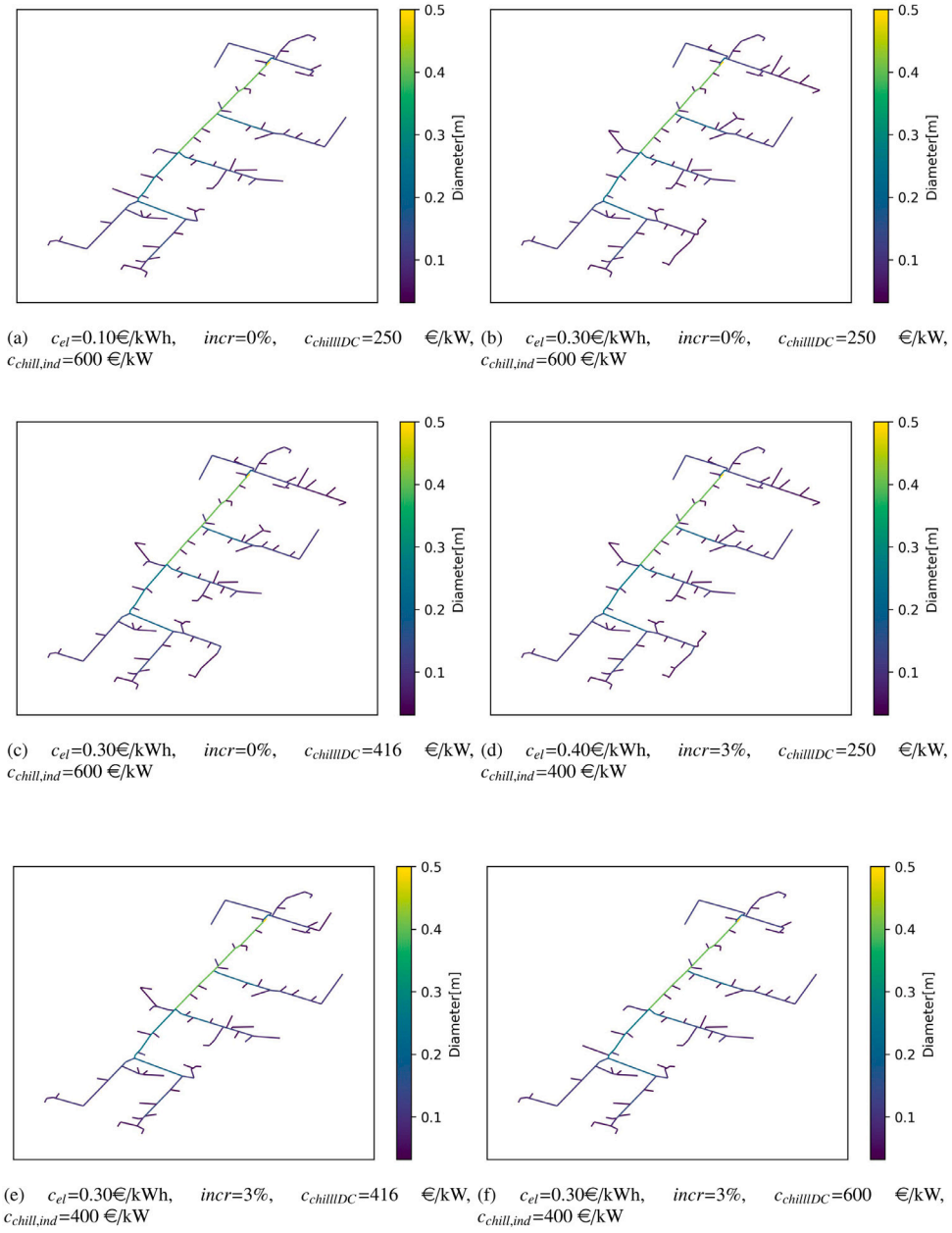

(a) c_{el}=0.10€/kWh, $incr$=0%, $c_{chillIDC}$=250 €/kW, $c_{chill,ind}$=600 €/kW (b) c_{el}=0.30€/kWh, $incr$=0%, $c_{chillIDC}$=250 €/kW, $c_{chill,ind}$=600 €/kW

(c) c_{el}=0.30€/kWh, $incr$=0%, $c_{chillIDC}$=416 €/kW, $c_{chill,ind}$=600 €/kW (d) c_{el}=0.40€/kWh, $incr$=3%, $c_{chillIDC}$=250 €/kW, $c_{chill,ind}$=400 €/kW

(e) c_{el}=0.30€/kWh, $incr$=3%, $c_{chillIDC}$=416 €/kW, $c_{chill,ind}$=400 €/kW (f) c_{el}=0.30€/kWh, $incr$=3%, $c_{chillIDC}$=600 €/kW, $c_{chill,ind}$=400 €/kW

Fig. 16. Second stage network designs for different scenarios according to rigid model.

4.6. Rigid model

In this part are presented the results obtained with the rigid version of the model, in which it is avoided the installation of new pipes in the second stage in the same branches where there are already pipes installed previously in the first stage. Fig. 15 shows the network that should be installed from the beginning according to this model. The topology is similar to the one of the previous model, but 50 buildings would be connected from the beginning, ten more with respect to the flexible formulation. However, in this case, the number of possible enhancements in the second stage is equal to seventeen, six less with respect to the flexible model formulation. Six of these are shown in Fig. 16.

Compared to the more flexible model, in this case the number of users connected in the second stage is sensibly lower. Indeed the maximum amount of connected buildings is 64, while in the flexible version it is 99.

Fig. 17 shows the topology of a network that represents the intersection of the networks obtained by the two models. This network therefore connects only the buildings that are connected in both solutions. In Figs. 17(a) and 17(b) the branches are coloured on the base of the diameter selected in the first stage by each model. It can be observed that for most of the edges, the diameter is the same in the two solutions. However, in some branches, rigid model selected a larger diameter. This is also shown more clearly in Fig. 17(c), where the branches in which the rigid model selects a larger diameter are highlighted. Indeed, the rigid model selects larger pipes, since no future pipe modifications are considered. In the subnetwork common to both solutions, the average pipe diameter selected by the rigid model is 158 mm, while the average one selected by the flexible model is 150 mm. The expected value of the cost obtained by the rigid model formulation is shown in Table 3 and is 0.4% higher than the one found previously. Hence, a greater flexibility would guarantee slightly larger savings.

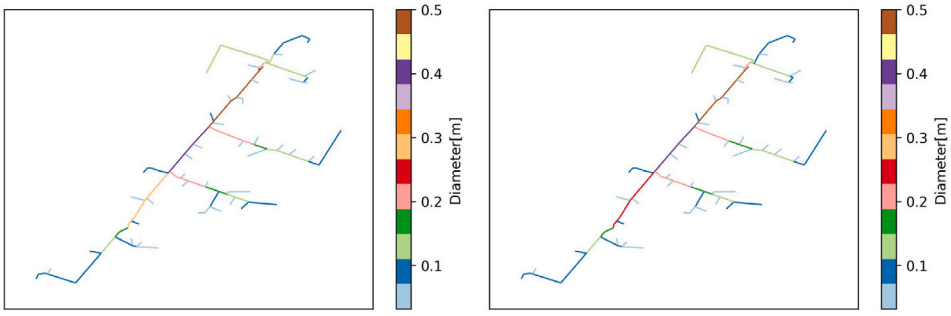

(a) Diameter selection at 1st stage in rigid model formulation

(b) Diameter selection at 1st stage in flexible model formulation

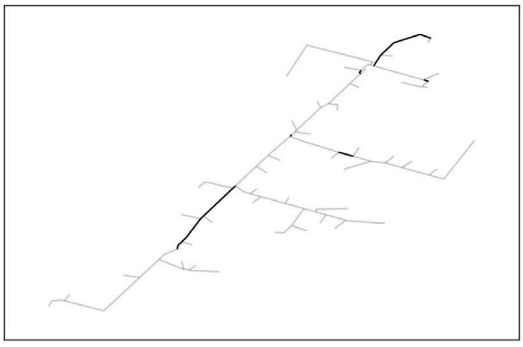

(c) Branches where rigid model selects larger diameters

Fig. 17. Comparison of diameter selection between rigid and flexible model solutions.

4.7. Impact of residual value of equipment

All previous results have been obtained by considering a positive cash flow due to the remainder life of equipment. Indeed, theoretically equipment that did not complete its life-time, can be used for new projects, such as a renovation of the district cooling system. However, it is also difficult to estimate the real residual value of partially worn-out parts. In this section, the results obtained by considering a null residual value of the equipment at the end of project life are presented. Fig. 18 shows the optimal first stage network obtained by the flexible model formulation. The initial number of connected users would be 44, 10% more than when considering residual value in the cost function. Depending on the scenario, the network can remain as it is or be enhanced in three different ways at the second decision stage, as shown in Fig. 19.

Fig. 20 shows the distribution of the number of new connections added in the second stage according to the scenarios. It can be observed that if no residual value of equipment is taken into account, the maximum number of new buildings connected in the second stage would be 13, while it would be 59, if residual value is considered in the cost function. Moreover, only in 6 cases out of 54, the network would be enhanced in the second stage, if residual value is not included in the cost function. If this is taken into account, the network would be expanded in the second stage, in 29 scenarios out of 54.

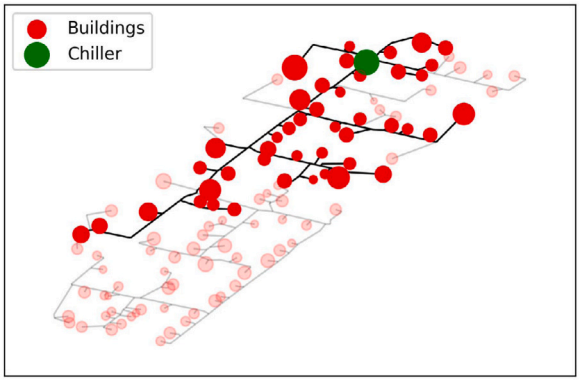

Fig. 18. Initial network layout if residual value is not taken into account.

5. Discussion

The results showed that it is more convenient to start with a smaller district cooling network and to enhance it in the future. In this way, the district cooling network can be enlarged if the demand or the electricity cost increases. At the same time, this solution limits the risks related to the possible future decrease of district cooling potential, by lowering the initial investment costs with the installation of a smaller network. From the analysis of the impact of the uncertainty on the optimal solution, it can be deduced that all the parameters affect the results. However, the electricity cost and the evolution of cooling demand are the ones with the highest impact. The comparison of the stochastic model with other deterministic approaches proved that the latter work better only if few specific scenarios occur, while on average they tend to provide 5% more expensive solution and three years larger payback time. Concerning the rigid model formulation, it proved to guarantee less flexibility, due to the impossibility to increase the flow capacity, by adding new pipes in the second stage in the same branches. Indeed, the number of possible network modifications is much lower with respect to the flexible formulation. In addition, the maximum number of users connected in the second solution is 35% smaller than in the first one. Moreover, the rigid model tends to install larger pipes from the beginning in order to be able to connect additional buildings in the second stage. The impact of the rigid formulation in terms of expected value of the cost function is limited to 0.4%.

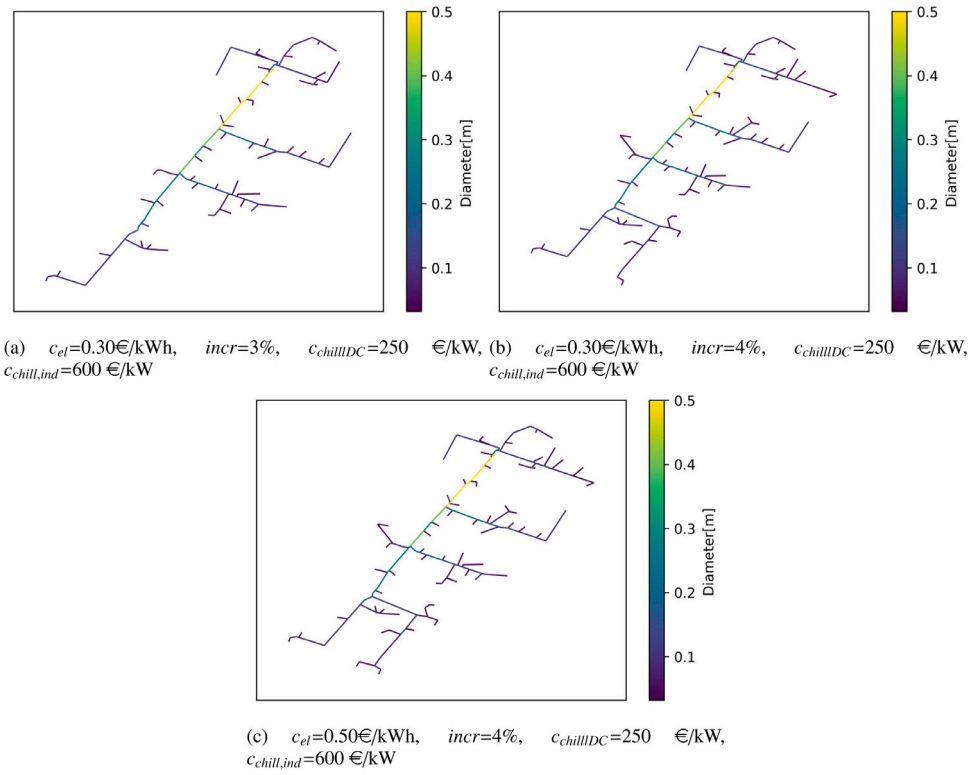

(a) c_{el}=0.30€/kWh, $incr$=3%, $c_{chillDC}$=250 €/kW, $c_{chill,ind}$=600 €/kW

(b) c_{el}=0.30€/kWh, $incr$=4%, $c_{chillDC}$=250 €/kW, $c_{chill,ind}$=600 €/kW

(c) c_{el}=0.50€/kWh, $incr$=4%, $c_{chillDC}$=250 €/kW, $c_{chill,ind}$=600 €/kW

Fig. 19. Possible network enhancement in the second stage if no residual value of equipment is considered.

Regarding the residual value of asset at the end of project life, if this is not taken into account in the cost function, the model tends to select a slightly wider network from the beginning. However, in 89% of the scenarios the network is not expanded in the second stage. Indeed, installing new pipes, substations or chillers in the second stage would mean using them for only half of their life if the residual value is not taken into account. Hence, the achievable operation savings would not be large enough to compensate the additional capital investment. The only scenarios in which the investment of new district cooling equipment is compensated by operation savings in the second time period, are the ones characterized by the highest potential of district cooling with respect to individual cooling. This result testifies that the value and the use of assets at the end of project life has a strong impact on the solution, influencing both first and second stage decisions.

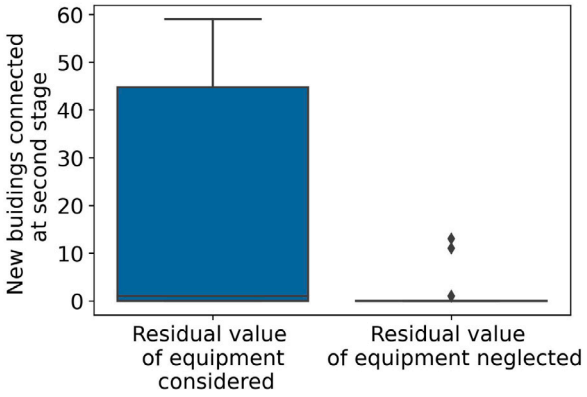

Fig. 20. Impact of residual value of equipment on second stage decisions.

6. Conclusion

In this paper a novel two-stage stochastic programming model for the design optimization of district cooling systems is presented. The optimization model is based on the mixed integer linear programming paradigm and all non-linear constraints have been linearized. The objective of the model is to determine the optimal initial design of a district cooling network and the future expansion for each possible scenario. The model optimizes the set of users to be connected both (a) immediately and (b) in the future on the base of the scenario conditions. A case study characterized by a neighbourhood of 108 buildings was used to test the tool. From the results it emerged that 40 buildings should be connected in the first design stage. In the second stage, depending on the scenario, the network can be either unchanged or enlarged in 23 different ways connecting up to 99 buildings. An analysis on the impact of the uncertainty was also performed. Among all parameters, electricity cost and increase rate of cooling demand are the ones that most influence the optimal solution. In particular, it was found that in 83% of the scenarios characterized by the lowest value of electricity cost, the network does not change in the second stage. Moreover, the impact of the stochastic approach was assessed by evaluating the cost under all possible scenarios and comparing it with other deterministic solutions. The two-stage stochastic programming model proved to be more robust than the others and, on average, it allows to reduce total costs by 5% with respect to deterministic methods that do not take into account uncertainty. In addition, stochastic model solution is characterized by three years lower payback time and 58% higher net present value. An alternative less flexible formulation of the model, called “rigid formulation”, has been implemented as well, in which the installation of multiple pipes in the same branches of the network (in order to increase flow capacity) is not allowed. The results showed, that the expected value of the solution obtained with this model is 0.4% larger than the one obtained with more flexible constraints. Moreover, the rigid model tends to install larger pipes and connect more buildings from the beginning, while less recourse actions are taken in the second stage. Lastly, it was analysed the impact of introducing or removing from the cost function the residual value of

assets at the end of project life. If this is not taken into account, in 89% of the cases, the model would not connect new buildings in the second stage, since the new installed equipment would be used for only part of their life-time and the achievable savings would not be large enough to compensate the supplementary capital investment. The developed models can be suitable to support decision makers in the different design phases of district cooling systems. Indeed, these systems should operate for a large time-horizon, where most of parameters are uncertain and could sensibly change in the long period. These models by taking into account the uncertainty of different parameters select a robust network design that can eventually be modified in the future, if conditions become more convenient for district cooling technology. At the same time, the robust network design allows to mitigate the risks related to a decrease of district cooling potential. The developed models enhance the potential of district cooling by properly handling the investment risks in the design phase. Future studies should take into account also the design and operation optimization of district cooling networks with thermal energy storage. In particular, the impact of uncertain electricity tariff on the optimal size of chillers and storages shall be investigated. In addition, future studies should focus on the optimal integration with other energy technologies, such as district heating systems or waste heat and solar energy through absorption chillers under different scenarios.

Declaration of competing interest

The authors declare that they have no known competing financial interests or personal relationships that could have appeared to influence the work reported in this paper.

Data availability

The data that has been used is confidential.

References

[1] L. Pérez-Lombard, J. Ortiz, C. Pout, A review on buildings energy consumption information, Energy Build. 40 (2008) 394–398, http://dx.doi.org/10.1016/J.ENBUILD.2007.03.007.

[2] L.C.M. Eberhardt, J. Rønholt, M. Birkved, H. Birgisdottir, Circular economy potential within the building stock - Mapping the embodied greenhouse gas emissions of four Danish examples, J. Build. Eng. 33 (2021) 101845, http://dx.doi.org/10.1016/J.JOBE.2020.101845.

[3] D. Ürge-Vorsatz, L.F. Cabeza, S. Serrano, C. Barreneche, K. Petrichenko, Heating and cooling energy trends and drivers in buildings, Renew. Sustain. Energy Rev. 41 (2015) 85–98, http://dx.doi.org/10.1016/J.RSER.2014.08.039.

[4] IEA, Cooling, IEA, Paris, 2021, URL https://www.iea.org/reports/cooling.

[5] IEA, The Future of Cooling, IEA, Paris, 2018, URL https://www.iea.org/reports/the-future-of-cooling.

[6] P.J. Ong, Y.Y. Lum, X.Y.D. Soo, S. Wang, P. Wang, D. Chi, H. Liu, D. Kai, C.-L.K. Lee, Q. Yan, J. Xu, X.J. Loh, Q. Zhu, Integration of phase change material and thermal insulation material as a passive strategy for building cooling in the tropics, Constr. Build. Mater. 386 (2023) 131583, http://dx.doi.org/10.1016/j.conbuildmat.2023.131583.

[7] G. Singh, R. Das, Comparative assessment of different air-conditioning systems for nearly/net zero-energy buildings, Int. J. Energy Res. 44 (2020) 3526–3546, http://dx.doi.org/10.1002/ER.5065, URL https://onlinelibrary.wiley.com/doi/full/10.1002/er.5065 https://onlinelibrary.wiley.com/doi/abs/10.1002/er.5065 https://onlinelibrary.wiley.com/doi/10.1002/er.5065.

[8] G. Singh, R. Das, Experimental study of a combined biomass and solar energy-based fully grid-independent air-conditioning system, Clean Technol. Environ. Policy 23 (2021) 1889–1912, http://dx.doi.org/10.1007/S10098-021-02081-4/TABLES/7, URL https://link.springer.com/article/10.1007/s10098-021-02081-4.

[9] G. Singh, R. Das, A novel variable refrigerant flow system with solar regeneration-based desiccant-assisted ventilation, Sol. Energy 238 (2022) 84–104, http://dx.doi.org/10.1016/J.SOLENER.2022.04.008.

[10] I. Dincer, A. Abu-Rayash, Community energy systems, Energy Sustain. (2020).

[11] H. Lund, S. Werner, R. Wiltshire, S. Svendsen, J.E. Thorsen, F. Hvelplund, B.V. Mathiesen, 4Th generation district heating (4GDH): Integrating smart thermal grids into future sustainable energy systems, Energy 68 (2014) 1–11, http://dx.doi.org/10.1016/J.ENERGY.2014.02.089.

[12] M. Jangsten, P. Filipsson, T. Lindholm, J.O. Dalenbäck, High temperature district cooling: Challenges and possibilities based on an existing district cooling system and its connected buildings, Energy 199 (2020) 117407, http://dx.doi.org/10.1016/J.ENERGY.2020.117407.

[13] A. Inayat, M. Raza, District cooling system via renewable energy sources: A review, Renew. Sustain. Energy Rev. 107 (2019) http://dx.doi.org/10.1016/j.rser.2019.03.023.

[14] E. Guelpa, V. Verda, Thermal energy storage in district heating and cooling systems: A review, Appl. Energy 252 (2019) 113474, http://dx.doi.org/10.1016/J.APENERGY.2019.113474.

[15] P.A. Østergaard, S. Werner, A. Dyrelund, H. Lund, A. Arabkoohsar, P. Sorknæs, O. Gudmundsson, J.E. Thorsen, B.V. Mathiesen, The four generations of district cooling - A categorization of the development in district cooling from origin to future prospect, Energy 253 (2022) 124098, http://dx.doi.org/10.1016/J.ENERGY.2022.124098.

[16] A.L. Chan, T.T. Chow, S.K. Fong, J.Z. Lin, Performance evaluation of district cooling plant with ice storage, Energy 31 (2006) 2750–2762, http://dx.doi.org/10.1016/J.ENERGY.2005.11.022.

[17] ASHRAE, District Cooling Guide, second ed., Atlanta, 2019.

[18] M. Jangsten, T. Lindholm, J.O. Dalenbäck, Analysis of operational data from a district cooling system and its connected buildings, Energy 203 (2020) 117844, http://dx.doi.org/10.1016/J.ENERGY.2020.117844.

[19] V. Eveloy, D.S. Ayou, Sustainable district cooling systems: Status, challenges, and future opportunities, with emphasis on cooling-dominated regions, Energies 12 (2019) 235, http://dx.doi.org/10.3390/en12020235.

[20] W. Gang, S. Wang, F. Xiao, D.C. Gao, District cooling systems: Technology integration, system optimization, challenges and opportunities for applications, Renew. Sustain. Energy Rev. 53 (2016) 253–264, http://dx.doi.org/10.1016/J.RSER.2015.08.051.

[21] K.M. Powell, W.J. Cole, U.F. Ekarika, T.F. Edgar, Optimal chiller loading in a district cooling system with thermal energy storage, Energy 50 (2013) 445–453, http://dx.doi.org/10.1016/J.ENERGY.2012.10.058.

[22] L. Wang, E.W. Lee, R.K. Yuen, A practical approach to chiller plants' optimisation, Energy Build. 169 (2018) 332–343, http://dx.doi.org/10.1016/J.ENBUILD.2018.03.076.

[23] W. Zhang, X. Jin, L. Zhang, W. Hong, Performance of the variable-temperature multi-cold source district cooling system: A case study, Appl. Therm. Eng. 213 (2022) http://dx.doi.org/10.1016/J.APPLTHERMALENG.2022.118722.

[24] Z. Chiam, A. Easwaran, D. Mouquet, S. Fazlollahi, J.V. Millás, A hierarchical framework for holistic optimization of the operations of district cooling systems, Appl. Energy 239 (2019) 23–40, http://dx.doi.org/10.1016/J.APENERGY.2019.01.134.

[25] S.J. Cox, D. Kim, H. Cho, P. Mago, Real time optimal control of district cooling system with thermal energy storage using neural networks, Appl. Energy 238 (2019) 466–480, http://dx.doi.org/10.1016/J.APENERGY.2019.01.093.

[26] K. Zaw, Z.Z. Kwik, W.Q. Chang, M.R. Islam, T.K. Poh, A techno-commercial decision support framework for optimal district cooling system design in tropical regions, Appl. Therm. Eng. 220 (2023) http://dx.doi.org/10.1016/J.APPLTHERMALENG.2022.119668.

[27] S. Mazzoni, B. Nastasi, S. Ooi, U. Desideri, G. Comodi, A. Romagnoli, The adoption of a planning tool software platform for optimized polygeneration design and operation – A district cooling application in south-east Asia, Appl. Therm. Eng. 199 (2021) http://dx.doi.org/10.1016/J.APPLTHERMALENG.2021.117532.

[28] A.C. Lo, P. Jones, F.W. Yik, Effects of pumping station configuration on the energy performance of district cooling systems, Build. Serv. Eng. Res. Technol. 38 (2017) 287–308, http://dx.doi.org/10.1177/0143624416680019.

[29] E. Guelpa, L. Bellando, A. Giordano, V. Verda, Optimal configuration of power-to-cool technology in district cooling systems, Proc. IEEE 108 (2020) 1612–1622, http://dx.doi.org/10.1109/JPROC.2020.2987420.

[30] A.L. Chan, V.I. Hanby, T.T. Chow, Optimization of distribution piping network in district cooling system using genetic algorithm with local search, Energy Convers. Manage. 48 (2007) 2622–2629, http://dx.doi.org/10.1016/J.ENCONMAN.2007.05.008.

[31] J. Zeng, J. Han, G. Zhang, Diameter optimization of district heating and cooling piping network based on hourly load, Appl. Therm. Eng. 107 (2016) 750–757, http://dx.doi.org/10.1016/J.APPLTHERMALENG.2016.07.037.

[32] J. Söderman, Optimisation of structure and operation of district cooling networks in urban regions, Appl. Therm. Eng. 27 (2007) 2665–2676, http://dx.doi.org/10.1016/J.APPLTHERMALENG.2007.05.004.

[33] F. Al-Noaimi, R. Khir, M. Haouari, Optimal design of a district cooling grid: structure, technology integration, and operation, Eng. Optim. 51 (2019) http://dx.doi.org/10.1080/0305215X.2018.1446085.

[34] A. Allen, G. Henze, K. Baker, G. Pavlak, Evaluation of low-exergy heating and cooling systems and topology optimization for deep energy savings at the urban district level, Energy Convers. Manage. 222 (2020) 113106, http://dx.doi.org/10.1016/J.ENCONMAN.2020.113106.

[35] A. Allen, G. Henze, K. Baker, G. Pavlak, N. Long, Y. Fu, A topology optimization framework to facilitate adoption of advanced district thermal energy systems, IOP Conf. Ser Earth Environ. Sci. 588 (2020) 022054, http://dx.doi.org/10.1088/1755-1315/588/2/022054.

[36] R. Yan, J. Wang, S. Zhu, Y. Liu, Y. Cheng, Z. Ma, Novel planning methodology for energy stations and networks in regional integrated energy systems, Energy Convers. Manage. 205 (2020) 112441, http://dx.doi.org/10.1016/J.ENCONMAN.2019.112441.

[37] T.T. Chow, A.L. Chan, C.L. Song, Building-mix optimization in district cooling system implementation, Appl. Energy 77 (2004) 1–13, http://dx.doi.org/10.1016/S0306-2619(03)00102-8.

[38] C. Bordin, A. Gordini, D. Vigo, An optimization approach for district heating strategic network design, European J. Oper. Res. 252 (2016) 296–307, http://dx.doi.org/10.1016/J.EJOR.2015.12.049.

[39] H. Bütün, I. Kantor, F. Maréchal, An optimisation approach for long-term industrial investment planning, Energies 12 (2019) 4076, http://dx.doi.org/10.3390/EN12214076.

[40] M. Wirtz, M. Heleno, H. Romberg, T. Schreiber, D. Müller, Multi-period design optimization for a 5th generation district heating and cooling network, Energy Build. 284 (2023) 112858, http://dx.doi.org/10.1016/j.enbuild.2023.112858.

[41] W. Gang, S. Wang, G. Augenbroe, F. Xiao, Robust optimal design of district cooling systems and the impacts of uncertainty and reliability, Energy Build. 122 (2016) 11–22, http://dx.doi.org/10.1016/j.enbuild.2016.04.012.

[42] G. Mavromatidis, K. Orehounig, J. Carmeliet, Design of distributed energy systems under uncertainty: A two-stage stochastic programming approach, Appl. Energy 222 (2018) 932–950, http://dx.doi.org/10.1016/J.APENERGY.2018.04.019.

[43] R.S. Lambert, S. Maier, J.W. Polak, N. Shah, Optimal phasing of district heating network investments using multi-stage stochastic programming, Int. J. Sustain. Energy Plan. Manag. 9 (2016) 57–74, http://dx.doi.org/10.5278/IJSEPM.2016.9.5, URL https://journals.aau.dk/index.php/sepm/article/view/1288.

[44] Z. Zhou, J. Zhang, P. Liu, Z. Li, M.C. Georgiadis, E.N. Pistikopoulos, A two-stage stochastic programming model for the optimal design of distributed energy systems, Appl. Energy 103 (2013) 135–144, http://dx.doi.org/10.1016/J.APENERGY.2012.09.019.

[45] N. Stevanato, F. Lombardi, G. Guidicini, L. Rinaldi, S.L. Balderrama, M. Pavičević, S. Quoilin, E. Colombo, Long-term sizing of rural microgrids: Accounting for load evolution through multi-step investment plan and stochastic optimization, Energy Sustain. Dev. 58 (2020) 16–29, http://dx.doi.org/10.1016/J.ESD.2020.07.002.

[46] J.R. Birge, F. Louveaux, Introduction to Stochastic Programming, Springer New York, New York, NY, 2011, http://dx.doi.org/10.1007/978-1-4614-0237-4.

[47] L.M. Pastore, G.L. Basso, L. de Santoli, Can the renewable energy share increase in electricity and gas grids takes out the competitiveness of gas-driven CHP plants for distributed generation? Energy 256 (2022) 124659, http://dx.doi.org/10.1016/J.ENERGY.2022.124659.

[48] Gestore Mercati Energetici, Esiti MGP, 2022, URL https://www.mercatoelettrico.org/it/download/DatiStorici.aspx.

[49] M. Swedblom, P. Mattson, A. Tvärne, H. Frohm, A. Rubenhag, District Cooling and the Customers' Alternative Cost, RESCUE, 2014.

[50] M.F. Jentsch, P.A. James, L. Bourikas, A.B.S. Bahaj, Transforming existing weather data for worldwide locations to enable energy and building performance simulation under future climates, Renew. Energy 55 (2013) 514–524, http://dx.doi.org/10.1016/J.RENENE.2012.12.049.

[51] A. Sciacovelli, V. Verda, R. Borchiellini, Numerical Design of Thermal Systems, CLUT, Turin, 2013.

[52] M. Neri, E. Guelpa, V. Verda, Design and connection optimization of a district cooling network: Mixed integer programming and heuristic approach, Appl. Energy 306 (2022) http://dx.doi.org/10.1016/j.apenergy.2021.117994.

[53] S.T. Taylor, Optimizing design and control of chilled water plants, ASHRAE J. (2011).